Guideline for Preliminary Sizing of a Vertical Take-Off and Landing System for Rigid-Wing Airborne Wind Energy

1 author:

Pirmin Sigron
ETH Zurich

1 PUBLICATION   **0** CITATIONS

Some of the authors of this publication are also working on these related projects:

Project   ftero - Airborne Wind Energy View project

Guideline for Preliminary Sizing of a Vertical Take-Off and Landing System for Rigid-Wing Airborne Wind Energy

Pirmin Sigron

Bachelor's thesis no. 19-048

Advisor: Sebastian Rapp (ext), Urban Fasel

IDMF - Laboratory of Composite Materials and Adaptive Structures
Prof. Dr. Paolo Ermanni
ETH Zürich

17.10.2019

ETH Zürich
IDMF - Laboratory of Composite Materials and Adaptive Structures
LEE O 203
Leonhardstrasse 21
8092 Zürich

Telefon: +41 (0)44 633 63 02

www.structures.ethz.ch

Abstract

Autonomous launching and landing of a tethered aircraft is one of the main challenges for an Airborne Wind Energy (AWE) system. A promising approach is Vertikal Take-Off and Landing (VTOL) with multiple rotors and many AWE startups rely on this take-off technique.

In this work the launching method VTOL is described using a mathematical model. This model can be used for a preliminary design regarding the size of the launching structure for a given AWE drone. In order to do so, important aircraft parameters are needed as an input and the required on-board power as well as the capacity of the energy storage are determined.

A critical requirement for an efficient power generation is a light-weight aircraft. Therefore, minimizing the weight of the VTOL system should be considered as one of the main objectives when designing the aircraft. In this work it is proposed to utilize the aerodynamic force to reduce the needed propeller thrust and hence minimize the required power for launching. Based on relevant equations describing the take-off procedure, a guideline for the design of such a VTOL system is presented.

To describe the launching sequence more accurately and investigate the effect of different flight paths on the needed thrust, a dynamic model is introduced and simulations on different start and landing sequences are carried out. Thereby, two control approaches are compared to each other focusing on the ability to optimally use the aerodynamic force to reduce the required propeller action. This leads to a recommendation of how the launch should be executed in order to be realizable with a light-weight VTOL system.

In this thesis it could be shown, that maximizing the aerodynamic force has a great potential regarding the reduction of the needed rotor thrust. This effect has not yet been investigated in the literature and should be considered when dealing with take-off and landing systems. Furthermore, it offers possibilities to novel control approaches, which optimally uses the aerodynamic force. The proposed control structure leaks in generality since it can only be applied in 2D models. Nonetheless, it gives an insight into the potential of using the aerodynamic force for control purposes.

Preamble

I am very grateful for all the support I encountered during the period of my bachelor thesis. First of all, I would like to thank my supervisors Sebastian Rapp and Urban Fasel for giving advice in a very motivating way and being easily reachable throught the work. Furthermore, sincere thanks are given to Prof. Paolo Ermanni for making the focus project ftero possible. Through his commitment for the students, he gave us the opportunity to realize an AWE system. Not to forget, a huge thank goes to the entire Focus Project ftero team for the pleasant atmosphere inside the team, your enormous commitment and the friendships made. Finally, I would like to deeply thank my family and friends for their continuous and encouraging support throughout the time span of this thesis and the whole bachelor studies.

Zurich, July 2019

Pirmin Sigron

ETH

Eidgenössische Technische Hochschule Zürich
Swiss Federal Institute of Technology Zurich

Department of Mechanical and Process Engineering
Institute of Design, Materials and Fabrication

ETH Zurich - CMAS

Leonhardstrasse 21

8092 Zurich, Switzerland

Student:	Pirmin Sigron	
	ETH-Nr: 16-927-931	Departement: MAVT
	Hochschule (if external student):	
Thesis:	Title: Design and Modeling of a Quadplane for Airborne Wind Energy	
	Kind of Thesis: Bachelor Thesis	Semester: FS 2019
Supervisor:	Prof. Dr. P. Ermanni	
Advisor:	Urban Fasel, Sebastian Rapp (TU Delft)	

Start of the work:	11.03.2019
Intermediate presentation (Zwischenpräsentation):	22.03.2019
Final presentation (Endpräsentation):	24.05.2019
Deadline delivery final report:	05.07.2019

Introduction

The third iteration of the focus project *ftero – Airborne Wind Energy (AWE) System* is currently carried out by eight students at CMASLab. The goal of this year's project is to develop an autonomous, power generating AWE System including a morphing capable aircraft. The team is developing an aerodynamically and structurally optimized aircraft of which the lift is used to drive a generator located on the ground station. To conduct the force to the ground, the aircraft is connected to the ground station by a tether. Further, different controllers have to be developed and optimized for the four main phases, namely traction, retraction, transition and vertical takeoff and landing (VTOL). Figure 1 shows a scheme of the AWE System.

The first two iterations pursued a tailsitting VTOL approach, using the two propellers in front of the aircraft and the flaps to stabilize hovering. This concept turned out to be vulnerable to disturbances, for example wind. Therefore, this year's team decided to add four propellers to the aircraft and pursuing a quadplane VTOL approach. The goal of the new approach is to improve control authority and robustness of the system. A reliable takeoff and landing

concept allows the team to carry out extensive testing which is essential for optimizing the system for power generation.
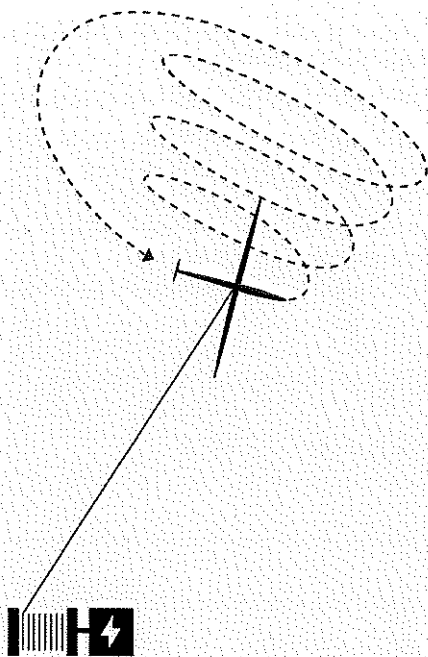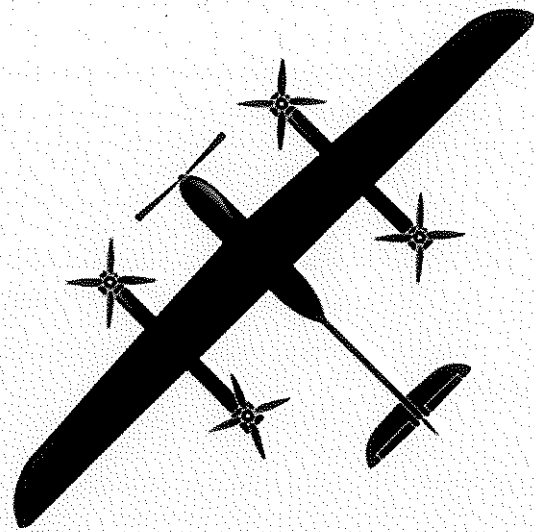

Figure 1: Scheme of the AWE System   Figure 2: Possible Design of the Quadplane

Objectives

The goal of this thesis is to investigate design methods for a quadplane VTOL system for AWE purposes, implementing a model in Matlab based on MILENA (VTOL aircraft of this year's project) and carry out simulations on hovering and transition phase.

In a first step, a methodology for the design of a quadplane VTOL systems is formulated and the quadplane VTOL concept is analysed regarding upscaling for AWE Systems. Further, a model of MILENA is implemented considering propeller dynamics. This model is used to carry out simulations of hovering and transition to horizontal flight mode.

The work done in this thesis can be used to analyse the suitability of the quadplane VTOL approach to different AWE Systems und carry out further researches on different control approaches to this VTOL concept. It also allows researches on alternative control concepts within traction, retraction and emergency stop.

Work breakdown

The work will be mainly subdivided in the following tasks:

1. Literature research
2. Formulating design methodology for quadplane VTOL
3. Analysis of upscaling of VTOL concept
4. Implementing model of MILENA in Matlab including propeller dynamics
5. Simulating hovering and transition to horizontal flight

6. Investigate design limitations of quadplane VTOL approach for AWE

The organization of the work is depicted in following table. The estimated deadlines are also shown.

Task	Week	11.03.2019	18.03.2019	25.03.2019	01.04.2019	08.04.2019	15.04.2019	22.04.2019	29.04.2019	06.05.2019	13.05.2019	20.05.2019	27.05.2019	03.06.2019	10.06.2019	17.06.2019	24.06.2019	01.07.2019
	Week	11	12	13	14	15	16	17	18	19	20	21	22	23	24	25	26	27
Task 1		▓	▓															
Task 2				▓														
Task 3					▓	▓												
Task 4							▓	▓	▓									
Task 5										▓	▓	▓	▓					
Task 6														▓	▓	▓	▓	▓
Intermediate presentation			█															
Final presentation												█						
Write report																█	█	█
Report deadline																		█

Bibliography

- Rapp, S., Schmehl, R., "Vertical Takeoff and Landing of Flexible Wing Kite Power Systems", Journal of Guidance, Control, and Dynamics, 2018
- Flores, G., Lozano, R. "Transition flight control of the quad-tilting rotor convertible MAV", 2013 International Conference on Unmanned Aircraft Systems, ICUAS 2013 - Conference Proceedings
- Cherubini, A., Papini, A., Vertechy, R., and Fontana, M., "Airborne Wind Energy Systems: A review of the technologies," Renewable and Sustainable Energy Reviews, vol. 51, 2015, pp. 1461–1476.
- Flores, G., Escareño, J., Lozano, R., et al., "Quad-tilting rotor convertible MAV: Modeling and real-time hover flight control", Journal of Intelligent and Robotic Systems: Theory and Applications, 2012

Please consider
- ❖ Directives and useful information about Student Projects at the Laboratory of Composite Materials and Adaptive Structures are available online at: http://www.structures.ethz.ch/content/dam/ethz/special-interest/mavt/design-materials-fabrication/composite-materials-dam/Education/Informationen/CMAS_Richtlinien_Studienarbeiten_EN.pdf
- ❖ Don't forget to register for the thesis under "My Studies" www.myStudies.ethz.ch at the begin of the semester

- ❖ This document has to be included in the final report

Zurich, 14/03/2019

Supervisor:	Advisor:	Student:
Prof. P. Ermanni	U. Fasel	P. Sigron

Contents

List of Figures

List of Tables

Abbreviations

AWE Airborne Wind Energy

ESC Electronic Speed Controller

FDM Fused Deposition Modeling

MILENA Morphing Intelligent Lightweight Extendable Novice Aircraft

NED North-East-Down

PLA Polylactide

UAVs Unmanned Aerial Vehicles

VTOL Vertikal Take-Off and Landing

List of symbols

α	[°]	Angle of attack
$\pm\alpha_0$	[°]	Cutoff angle
β	[°]	Sideslip angle
γ_a	[°]	Air-path inclination angle
$\delta_s c$	[ ]	Scaling factor for flight path construction
ε	[°]	Elevation angle
η	[ ]	Propeller efficiency
θ	[°]	Pitch angle
λ_W	[°]	Wind angle
μ_e	$[\frac{kJ}{kg}]$	Energy density of energy storage
μ_p	$[\frac{kW}{kg}]$	Power density of power train
ν	[°]	Rotor tilt angle
ρ	$[\frac{kg}{m^3}]$	Air density
σ	[ ]	Blending function
τ	$[s]$	Time constant of filter
ϕ	[°]	Roll angle
chi_a	[°]	Air-path azimuth angle
ψ	$[m^2]$	Wing area
a_{cmd}	$[\frac{m}{s^2}]$	Desired acceleration
A_{prop}	$[m^2]$	Propeller disk area
c	$[m]$	Chord length
C_D	[ ]	Drag coefficient
C_{D0}	[ ]	Constant drag coefficient
C_{Da}	$[\frac{1}{rad}]$	First order drag coefficient
C_L	[ ]	Lift coefficient
C_{L0}	[ ]	Constant lift coefficient
C_{La}	$[\frac{1}{rad}]$	First order lift coefficient
d	$[m]$	Wing span
D	$[m]$	Propeller diameter
F_a	$[N]$	Aerodynamic force
F_{cmd}	$[N]$	Desired force
F_D	$[N]$	Drag force
F_g	$[N]$	Gravitational force
F_k	$[N]$	Net force acting on kite
F_L	$[N]$	Lift force
F_P	$[N]$	Propeller force
F_t	$[N]$	Tether force
g	$[\frac{m}{s^2}]$	Gravitational constant
h_t	$[m]$	Target height
K_I	[ ]	Integrator feedback gain
K_P	[ ]	Proportional feedback gain

m	$[kg]$	Total aircraft mass
m_e	$[kg]$	Mass of energy storage
m_k	$[kg]$	Kite mass (without VTOL)
m_p	$[kg]$	Mass of propulsion unit
m_{vtol}	$[kg]$	Mass of VTOL system
M	$[\ ]$	Transition rate
n	$[\ ]$	Number of propellers
P_{fl}	$[m]$	Flight path vector
P_{ob}	$[kW]$	On-board power
s	$[\ ]$	safety factor
SCM	$[m]$	Standard mean chord
T	$[N]$	Thrust
V'	$[\frac{m}{s}]$	Effective airspeed at propeller
v_{cmd}	$[\frac{m}{s}]$	Desired velocity
v_i	$[\frac{m}{s}]$	Induced velocity
$v_{path,k}$	$[\frac{m}{s}]$	Kinematic path velocity
v_{wind}	$[\frac{m}{s}]$	Wind speed
v_{6m}	$[\frac{m}{s}]$	Wind speed at $6m$ above ground level
w_l	$[\frac{kg}{m^2}]$	Wing loading of aircraft without VTOL system
$w_{l,tot}$	$[\frac{kg}{m^2}]$	wing loading of entire aircraft including VTOL system
X_k	$[m]$	Position of aircraft
X_{proj}	$[m]$	Projected position of aircraft
X_{rel}	$[m]$	Relative position of aircraft
X_{tar}	$[m]$	Target point
X_w	$[m]$	Waypoint
X_0	$[m]$	Start point of launching sequence

1 Introduction

The need for electric energy in today's globalized world is vastly growing. To cope with the high demand and replace conventional energy sources like fossil fuel or coal, that have a harming impact on the environment, sustainable energy sources must be exploited. Wind has the potential to play an important role in the sustainable energy production of the future. To provide access to the entire potential of this source, high altitude winds that are stronger and steadier than ground level winds must be utilized for energy production[5],[6].

AWE gives the possibility to harvest these winds in high altitudes. In addition, compared to conventional wind turbines it needs drastically less constructive material and it's independent from the ground conditions at the operation site. These advantages enable the technology to compete with low-cost conventional energy sources and take a major role in energy supply [7].

In the last decades a lot of research in the field of AWE was carried out. As a result numerous startups arose with many different concepts how to efficiently harvest high altitude winds [8], [5]. An AWE system is composed of an airborne drone, a ground unit and a tether connecting the two main parts. Today's AWE systems can be classified into (i) ground generating and (ii) fly generating power plants. In the case of ground generating systems the conversion of kinetic into electric energy takes place on the ground unit, whereas fly generating power plants convert the energy on the aircraft from which electrical energy is than transmitted to the ground unit using conductive tethers. When the kite is flying in crosswind motions it is referred to as a cross wind AWE system. Ground generating as well as fly generating cross wind concepts have been introduced [8],[4],[2]. For ground generating cross wind systems the kite's high lift force is used to pull a tether connected to the ground station. This tether force can further be used for power generation on the ground unit by driving an electric generator [5],[8].

This thesis was realized with the background of the student project *ftero - Airborne Wind Energy System* where a fixed-wing cross wind AWE system was developed and manufactured mainly using carbon fibre and 3D-printed Polylactide (PLA) components using the Fused Deposition Modeling (FDM) method. For the prototype of the third iteration of the project (2019) the VTOL launching approach was implemented, which is going to be investigated in this thesis. Therefore, when using aircraft parameters it is referred to the most recent prototype Morphing Intelligent Lightweight Extendable Novice Aircraft (MILENA) of the ftero project, which is depicted in figure 1 [9].

As mentioned before, a major challenge for AWE systems is autonomous launching and landing of the aircraft. The takeoff and landing concept must meet the following three requirements: (i) ability to launch in limited space so it can be operated at varying sites, (ii) a lightweight structure, (iii) low complexity so the launch and landing is robust and reliable. Regarding cross wind AWE systems the additional mass is an important criteria since it must be carried during all flight phases. This reduces not only controllability and maneuverability of the system, but also efficiency of power generation [10],[11].

The three mainly proposed take-off and landing strategies are: (i) rotational take-off, (ii) linear take-off with on-board propellers and (iii) the here described VTOL with rotors. Although, some research was conducted on the viability of these different systems and the linear take-off was proposed to be the most viable, [10] no clear trend towards a specific concept can be deduced when analysing the pursued approaches. Nonetheless, many companies rely on VTOL

Figure 1: Prototype of focusproject ftero with four propellers for VTOL

with propellers. Taking into account this, the thesis aims to introduce a design guideline for an efficient VTOL systems with multiple rotors. For that, well-known physical principles are used to describe the system and the dependency of the needed on-board power on different flight parameters. To consider changing conditions during the ascent and to analyse simple control approaches, a basic dynamic model is introduced and simulations on different start sequences are carried out. This is done aiming to optimally use the aerodynamic forces to reduce the needed rotor thrust. That way, a recommendation for the design of a VTOL structure for a given AWE kite can be given, including a guideline for the start procedure.

2 State-of-the-art

Due to the critical requirement for a cross-wind AWE system of autonomously launching and landing a tethered aircraft, different concepts have been introduced and implemented. As highlighted in the introduction, three promising approaches have been investigated intensively [11].

Rotational take-off

This concept consists of a rotating ground unit with a launching arm. The tip of the launching arm serves as a mount for the kite during the first period of the landing procedure. The aircraft is accelerated in a circular motion around the ground station until it reaches stall speed. Than the aircraft leaves the supporting arm and gains height until operation altitude is reached.
For landing, the aircraft tracks a circular path around the ground unit, which follows the pattern rotating around its axes. The aircraft is then retracted using the tether until it reaches the mounting of the launching arm.
The rotational take-off was implemented by EnerKite and simulations on the start and landing procedure have been carried out within the Master's Thesis of Elke Boenteke [1],[11]. The main advantage of this concept is that no additional mass has to be add to the kite since no on-board propulsion is needed in optimal case. The large ground area which is required during launch and landing because of the circular motion as well as the complexity of the system are drawbacks [10].

Linear take-off with on-board propellers

The linear take-off can also be referred to as a catapult-start. Similar to the rotational take-off, mainly an external power source is used to accelerate the aircraft in such a way that it reaches stall speed and can be controlled using control surfaces. It can be thought of different accelerating systems, like linear motors, springs, rubber bands or the winch of the base unit itself. The on-board propellers can be used to sustain the forward speed during ascent to the operational altitude and to ensure proper maneuverability [12]. This approach was implemented by the company Ampyx Power using a linear motor [2]. Carrying out viability analysis on different launching systems, linear take-off with on-board propellers were proposed to be the most promising approach [10].
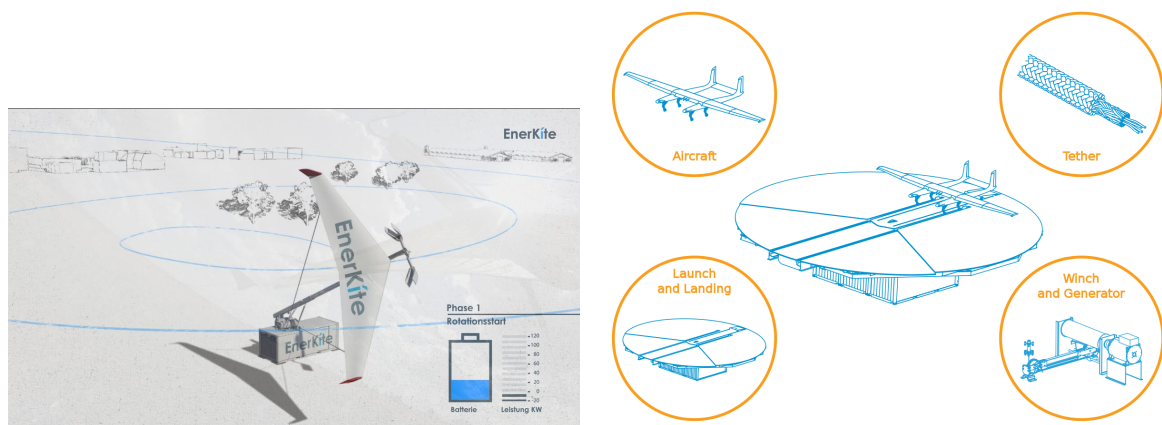

Figure 2: (a) Rotational take-off implemented by EnerKite [1], (b) linear take-off with rotors employed by Ampyx Power [2]

Vertical take-off with rotors

Here, the aircraft is equipped with multiple propellers pointing in vertical direction. Similar to a multicopter, this allows the kite to hover in a given position. Since controllers for multicopters are well-proven and readily available, this approach can be easily implemented. The VTOL approach requires little space and can be carried out independently of the ground conditions at the operation site [13],[14]. The main drawback is the relatively high additional mass for the launching system. This is why a vertical take-off with rotors was proposed to be less viable than the linear take-off [10].

VTOL was employed by different ground-generating companies like TwingTec, Kitemill, e-kite or KiteX but also by Makani Power for launching and landing their on-board generating system [3],[4],[15],[16],[17]. In figures 3a and 3b the AWE systems developed by Twingtec and Makani Power can be seen.

Figure 3: (a) Cross-wind AWE system emloying VTOL from TwingTec [3], (b) on-board generating system using VTOL developed by Makani Power [4]

Design Methodology for Aerial Vehicles

Based on mathematical descriptions of the investigated system, divers design guidelines have been introduced for different aerial vehicles. Because of the increasing importance of Unmanned Aerial Vehicles (UAVs) not only in leisure activities but also for industrial applications such as inspection, agriculture and transportation, the design of such drones are particularly well documented [18],[19]. Thereby, the selection of the most important components of vehicle is done based upon the analysis of the system's behavior on changing parameters. Models for the different sub systems are introduced with the aim of finding a representation of chosen design parameters based on given environmental conditions as well as on constraints defined for the system. In a further step, methods were introduced to optimize the system regarding selected properties. This has been done analytically as well as by means of experiments [20],[21].

In the field of AWE for instance, optimizations of the flight trajectory in real time [22] or a method for optimal experimental design of the AWE system have been introduced [23]. Regarding the launching and landing concept, the viability of different start and landing systems have been analysed and compared to each other, but no design methodology of the proposed start and landing systems can be found in the literature.

3 Modelling of a VTOL System

In order to describe the behavior of a rigid-wing AWE system employing VTOL, the system has to be described mathematically. After the definition of the used coordinate systems and the equations required to describe the system, first a static model is introduced which can be used for preliminary sizing considerations when designing a VTOL system. In a second step, a dynamic model is introduced in order to describe the system more accurately considering control actions and controllability. The final goal is to find a lightweight solution of the power train and the energy storage that can be used for a given AWE aircraft.

3.1 Definitions and Equations Describing the System's Components

3.1.1 Notation

When describing velocities and vectors related to aeronautics different reference systems and coordinate frames must be used. In (3.1 - 3.3) the notational convention that is used throughout the entire thesis is shown.

- Position vector:

$$X = \begin{pmatrix} x & y & z \end{pmatrix}^T \tag{3.1}$$

- Velocity vector:

$$V = \begin{pmatrix} u & v & w \end{pmatrix}^T \tag{3.2}$$

- Forces:

$$F = \begin{pmatrix} F_x & F_y & F_z \end{pmatrix}^T \tag{3.3}$$

Velocities relative to the inertial coordinate system are referred to *kinematic velocities* and denoted with a subscript $_k$. For velocities relative to the air (*airspeed*) the subscript $_a$ is used. If no subscript is present it is referred to the airspeed.

To denote the coordinate systems superscripts are used (see following section).

3.1.2 Coordinate Systems

The calculations done in this thesis require the definition of several coordinate systems. In table 1 an overview of the frames used is given.

North-East-Down (NED) Frame

The usual choice for the inertial coordinate system is the NED system, where the x-axis is pointing through north, the y-axis through east and the z-axis is completing the right-handed set. In this thesis the NED-frame is denoted by the superscript O [24],[25].

Wind Frame

The wind frame is defined by the wind direction. Since in this work only horizontally blowing wind is considered, the x-axis and y-axis always form a horizontal plane. For giving an intuitive representation, the z-axis of the wind frame is pointing upwards, unlike the one of the NED-frame.

Name	Origin	Directions
NED $\equiv O$	ground station	(e_x^O = north, e_y^O = east, e_z^O = down)
Wind $\equiv W$	ground station	(e_x^W = wind direction, e_z^W = up)
Body-fixed $\equiv B$	center of mass of aircraft	(e_x^B = forward, e_y^B = right, e_z^B = down)
Aerodynamic $\equiv A$	center of mass of aircraft	(e_x^A, e_y^A, e_z^A) (see description in 3.1.2)
Rotor $\equiv R$	center of mass of aircraft	($e_x^R, e_y^R = e_y^B, e_z^R$ = negativ thrust direction)

Table 1: Different coordinate systems used for calculations.

Body-fixed Frame

Here the x-axis is pointing in longitudinal direction of the aircraft (along fuselage, from tail to front) and is therefore denoted as *forward*. The y-axis is pointing to the tip of the right-hand wing and the z-axis completes the right handed system.

Aerodynamic Frame

To describe the aerodynamic forces occurring during flight, a aerodynamic air frame is defined. This way, the x-axis is pointing through the airspeed vector which is defined as the velocity of the aircraft relative to the surrounding air. The frame's y- and z-axis are defined using the angle of attack α and the side slip angle β as described in section 3.1.3.

Rotor Frame

This frame has been introduced to facilitate the use of a rotor tilt angle ν. Since the propellers are constraint to rotate around the body-fixed y-axis, it is equivalent to the y-axis of the rotor frame.

3.1.3 Transformations

In the following section, the transformations between the different coordinate systems are introduced including the definition of all relevant angles.

- W - O: Since the wind is assumed to blow horizontally the wind angle λ_W, suffices to describe the transformation from W- into NED-frame

$$M_{OW} = \begin{pmatrix} \cos \lambda_W & \sin \lambda_W & 0 \\ \sin \lambda_W & -\cos \lambda_W & 0 \\ 0 & 0 & -1 \end{pmatrix}. \tag{3.4}$$

- B - O: The transformation from B- to NED-frame is defined by the Euler angles using the

ZYX rotation order

$$M_{OB} = M_{O1}(\psi)M_{12}(\theta)M_{2B}(\phi) \begin{cases} Yaw \equiv \psi & \text{rotating around } e_z^O\text{- axis} & \to M_{O1}(\psi) \\ Pitch \equiv \theta & \text{rotating around } e_y^1\text{- axis} & \to M_{12}(\theta) \\ Roll \equiv \phi & \text{rotating around } e_x^2\text{- axis} & \to M_{2B}(\phi) \end{cases}.$$

- A - B: The aerodynamic frame is defined using the angle of attack and the sideslip angle, where α is defined positive for a negative rotation around the body-frame y-axis and β is defined positive for a positive rotation around the body-frame z-axis

$$\alpha = \arctan(\frac{w_a^B}{u_a^B}) \tag{3.5}$$

$$\beta = \arcsin \frac{v_a^B}{|V_a|}. \tag{3.6}$$

For the transformation from the aerodynamic frame to the body-fixed frame the following rotational matrix results (rotation order: $-\beta$, α)

$$M_{BA} = \begin{pmatrix} \cos\alpha\cos\beta & -\cos\alpha\sin\beta & -\sin\alpha \\ \sin\beta & \cos\beta & 0 \\ \sin\alpha\cos\beta & -\sin\alpha\sin\beta & \cos\beta \end{pmatrix}. \tag{3.7}$$

- O - A: For a direct transformation from the NED- to the aerodynamic frame the *air-path azimuth angle* χ_a and *air-path inclination angle* γ_a can be used. They are defined using the airspeed V_a as it can be seen in. In this work the *air-path bank angle* is assumed to be zero [26]. For the transformation matrix from the NED to the aerodynamic airframe the following matrix can be deduced (rotation order: χ_a, γ_a) [24]

$$M_{AO} = \begin{pmatrix} \cos\gamma_a\cos\chi_a & \cos\gamma_a\sin\chi_a & -\sin\gamma_a \\ -\sin\chi_a & \cos\chi_a & 0 \\ \sin\gamma_a\cos\chi_a & \sin\gamma_a\sin\chi_a & \cos\gamma_a \end{pmatrix}. \tag{3.8}$$

- B - R: This transformation corresponds to a rotation around the body frame y-axis and can therefore be described by the rotor tilt angle ν. The transformation matrix from B to R is analogue to M_{12} defined as

$$M_{RB} = \begin{pmatrix} \cos\nu & 0 & -\sin\nu \\ 0 & 1 & 0 \\ \sin\nu & 0 & \cos\nu \end{pmatrix}. \tag{3.9}$$

3.1.4 Given Parameters

To assure the methodology can be used for any aircraft, some important parameters are assumed to be given. These are the wing area A and the wing loading w_l. The wing loading is defined as the fraction of the aircraft's weight and it's wing area

$$w_l = \frac{m_k}{A}. \tag{3.10}$$

In case the wind loading is not given one can approximate it with available data from different AWE systems to be $w_l = 13.26 \frac{kg}{m^2}$ (Figure 4) [9],[15],[11].
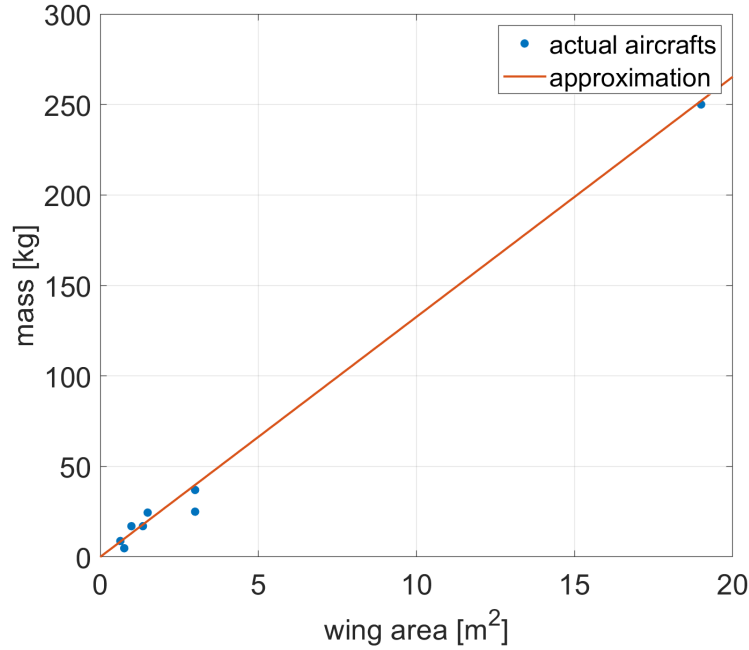
Figure 4: Wing loading of different AWE aircrafts

3.1.5 Mathematical Description of Components

In order to analyse the launching procedure numerically and find a lightweight solution for the VTOL components of a given kite, the system has to be described mathematically. This is done by introducing equations that characterize the important elements of the take-off system and defining relevant models.

Mass

The total mass of the aircraft can be split in different sub masses

$$m = m_k + m_p + m_e. \tag{3.11}$$

Where m_k is the mass of the kite, m_p is the mass of the propulsion unit (that is the drive train) and m_e is the mass of the energy storage. Here m_k incorporates all the aircraft's components besides the VTOL structure like the fuselage, the rear, a drive train mounted in horizontal direction, the actuation components for control surfaces etc.

The masses of the propulsion and of the energy storage can be related to the on-board power P_{ob} as follows

$$m_p = \frac{P_{ob}}{\mu_p} \tag{3.12}$$

$$m_e = \frac{2P_{ob}h_t}{\mu_e w_k^W}. \tag{3.13}$$

Where μ_p and μ_e are the power and energy density of the respective system. Here h_t denotes

the target height and w_k^W vertical velocity during the start procedure. The factor 2 in the formula for m_e accounts for the energy needed for the landing procedure, which is proposed to be a corresponding descent following the same trajectory as for the launch.

The power density of the drive train is taken from market surveys from heavy lift UAVs [19]. In figure 5a the relation between the mass and the maximal continuous power of considerable motors can be seen. For the energy density data from commonly used lithium-ion polymer batteries are used. The approximated energy density curve is depicted in figure 5b [27]. For the mass of the energy storage the provided power of the batteries is not considered because today's lithium-ion batteries are able to deliver higher peak power values than needed [14]. Both, the power and energy density are expected to increase in the next decades [28].

The mass of the entire VTOL structure can be denoted by the sum of the propulsion unit and the energy storage

$$m_{vtol} = m_p + m_e, \tag{3.14}$$

and therefore corresponds to the main matter of interest when designing the VTOL system of an AWE aircraft.
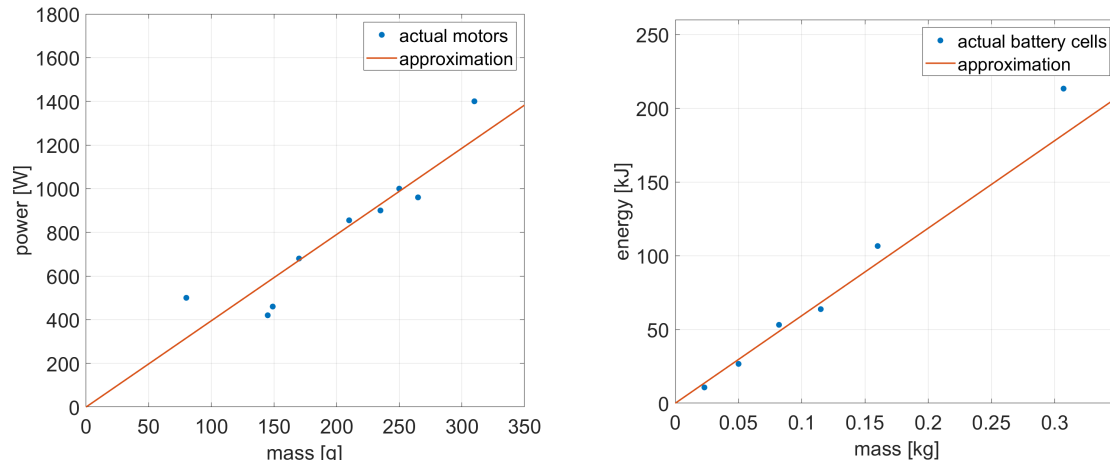
Figure 5: (a) Power of heavy lift UAVs, (b) Energy density of lithium-ion batteries

Momentum Theory in Oblique Flow

The thrust produced by the rotating propellers can be described with the Actuator Disk Theory which is based on the momentum conservation. (cite theys oblique flow, Harlock aktuator disk theory) The resulting equation for the thrust is

$$T = \frac{1}{2}\rho A_{prop}(v_{out}^2 - v_{in}^2). \tag{3.15}$$

Where ρ is the air density, A_{prop} is the propeller area, v_{in} and v_{out} the velocity of the incoming respectively outgoing airflow. This theory is adequate for general horizontal flight, where the relative airflow is aligned with the propeller's rotation axes. In case of a multicopter hovering in windy conditions like it is assumed for a start of an AWE aircraft, one has to account for the direction of the relative airspeed. The Actuator Disk Theory can be expanded for oblique flow according to [25]

$$T = 2\rho A_{prop}V'v_i. \tag{3.16}$$

Where v_i is the induced velocity and V' describes the effective speed of the flow at the rotor

$$V' = \sqrt{(u^B)^2 + (v^B)^2 + (w^B - v_i)^2}. \tag{3.17}$$

For the given V' the rotor's thrust directs along the body's negative z-axis like it is the case for a rotor tilt angle of $\nu = 0°$ in our VTOL system. When the rotors are tilted, the calculations must be carried out in the rotor frame but remain valid.

With the same momentum theory an expression for the power needed to produce a given thrust can be derived

$$P = T(v_i - w^B). \tag{3.18}$$

For a given thrust T, equations 3.16 and 3.18 can be solved numerically to receive the induced velocity v_i as well as the required power P.

Aerodynamic Forces

In the case of hovering in horizontal position like it is the case for the investigated VTOL approach, the aerodynamic forces can not be neglected. Namely the aerodynamic lift and drag force pointing in negative z- respectively negative x-axis of the aerodynamic airframe. The two forces can be described as follows [29]

$$F_D = \frac{1}{2}C_D\rho|V_a|^2A, \tag{3.19}$$

$$F_L = \frac{1}{2}C_L\rho|V_a|^2A, \tag{3.20}$$

$$F_a^A = \begin{pmatrix} -F_D \\ 0 \\ -F_L \end{pmatrix}, \tag{3.21}$$

where F_a^A denotes the aerodynamic force, C_D and C_L are the drag and the lift coefficient and $|V_a|$ is the magnitude of the aerodynamic velocity.

For the drag coefficient a commonly used first order approximation in α was implemented taking C_{D0} and C_{Da} from the aerodynamic analysis of MILENA with *XFLR5* [30]

$$C_D = C_{D0} + \alpha C_{Da}. \tag{3.22}$$

This approximation is considered to be sufficient because the drag plays a minor role and is hard to estimate for large angles of attack.

To account for the effect of stall, a model that approximates the lift coefficient as the one of a flat plate for very large and small (negative) angles of attack, is used. The effect can be seen in 6 and the corresponding equations are given by

$$C_L = (1 - \sigma)(C_{L0} + C_{La}\alpha) + \sigma(2sign(\alpha)\sin\alpha^2 cos\alpha) \tag{3.23}$$

where

$$\sigma = \frac{1 + e^{-M(\alpha-\alpha_0)} + e^{M(\alpha+\alpha_0)}}{(1 + e^{-M(\alpha-\alpha_0)})(1 + e^{M(\alpha+\alpha_0)})}. \tag{3.24}$$

The transition rate M and the cutoff angles $\pm\alpha_0$ must be found by trial and error to meet the

actual lift coefficient as good as possible.
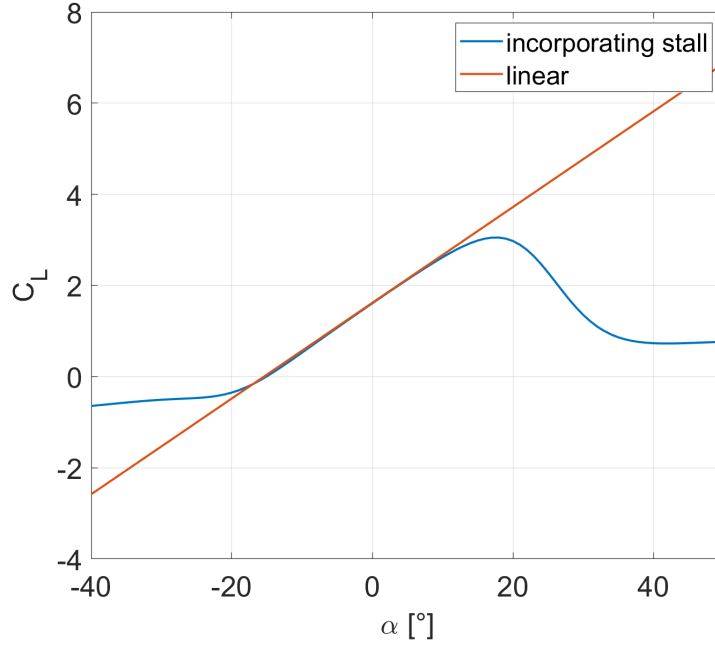
Figure 6: Lift model incorporating the effects of stall for C_L compared to linear model

3.2   Mathematical Model

The previously described principles are now used to create a mathematical model that can be used for numerical analysis of the launch sequence. The goal is to investigate the needed power and the associated mass of the VTOL structure for different environmental conditions and trajectories.

3.2.1   Inputs to the Model

Wind
For the static model a uniform wind shear profile is used. The wind direction λ_W and the wind speed v_{wind} must be given to the model as an input.

Trajectory
For the evaluation a stationary and rectilinear ascent with prescribed advance velocity is assumed. The inputs are given using the elevation angle ε and the kinematic path velocity $v_{path,k}$. The elevation angle is defined as a negative rotation around the wind frame's y-axis and defines the inclination angle of the flight path

$$
\left.
\begin{aligned}
0° < \quad \varepsilon \quad < 90° \quad &\to \quad \text{flying backwards in wind direction} \\
90° < \quad \varepsilon \quad < 180° \quad &\to \quad \text{flying forward against wind direction}
\end{aligned}
\right\} \text{elevation angle } \varepsilon.
$$

With these inputs the kinematic velocity of the aircraft can be defined as follows

$$
v_k^W = \begin{pmatrix} \cos(\varepsilon) v_{path,k} \\ 0 \\ \sin(\varepsilon) v_{path,k} \end{pmatrix}. \tag{3.25}
$$

Orientation of Aircraft

Since in 2D case the side slip angle is assumed to be zero, it is proposed to always align the aircraft in wind direction in order to optimally use the wind for lift production. That way, the yaw-angle ψ is given by the wind angle λ_W as

$$
\begin{aligned}
\text{for} \quad 0° \leq \; \lambda_W < 180° \; &\rightarrow \; \psi \equiv \lambda_W + 180° \\
\text{for} \quad 180° \leq \; \lambda_W < 360° \; &\rightarrow \; \psi \equiv \lambda_W - 180°
\end{aligned}
.
$$

and varying the orientation of the aircraft is limited to the pitch angle θ.

3.2.2 Static Model

To compute the required on-board power for hovering, the necessary thrust has to be known. Due to the assumption of a stationary ascent, a force balance can be formulated and solved for the rotor thrust. In the given model the only forces acting on the aircraft are the gravitational force F_g and the aerodynamic force F_a. The tether force is assumed to be zero since it is proposed to hold it loose throughout the launch.

Gravitational Force

The mass can be written according to the model introduced in section 3.1.5 as

$$
m = \mu_k A + \left(\frac{1}{\mu_p} + \frac{2h_t}{\mu_e w_k^O} \right) P_{ob}. \tag{3.26}
$$

Since the gravitational force always directs along the z-axis of the NED frame it can be defined as

$$
F_g^O = \begin{pmatrix} 0 \\ 0 \\ mg \end{pmatrix}. \tag{3.27}
$$

Aerodynamic Force

Following the explanations in section 3.1.5 the aerodynamic forces occurring during launch can be determined with the knowledge of the airspeed v_a^A and the aircraft characteristics, namely the wing area A as well as the lift and drag coefficients C_L and V_D. The aerodynamic force can be written as

$$
F_a^A = \begin{pmatrix} -F_D \\ 0 \\ -F_L \end{pmatrix}. \tag{3.28}
$$

Thrust

Assuming the x-component of the aerodynamic force in O-frame and other disturbances as well as the thrust needed for control actions to be negligible, the force balance in NED-frame's z-direction reads

$$
T = mg + F_{a,z}^O, \tag{3.29}
$$

where T is the needed thrust for hovering.

On-Board Power

Inserting the thrust into equations 3.16 and 3.18 leads to the following representation

$$P_{ob} = (v_i - w^B)(mg + F_{a,z}^O)\frac{s}{\eta} \tag{3.30}$$

$$2\rho A_{prop}V'v_i = (mg + F_{a,z}^O)\frac{s}{\eta}. \tag{3.31}$$

Here s denotes a safety factor and η accounts for the propeller efficiency not to be 100%. It is important to see, that the mass m is a function of P_{ob}. Therefore, this system must be numerically solved for the on-board power and the induced velocity P_{ob} and v_i. The result can then be inserted into equation 3.26 to get the corresponding total mass and into equations 3.12 and 3.13 to compute the mass of the VTOL system.

3.2.3 Parametrisation of Propeller Area

Since the thrust outcome strongly dependens on the propeller area A_{prop} and to prevent unfeasible results, the propeller area is parametrized setting the propeller diameter D to $\frac{3}{4}$ times the chord length c. This ratio is suggested for a quadplane configuration, meaning four rotors installed in vertical direction. The chord can be described using the wing area and a given aspect ratio

$$\lambda = \frac{d}{SMC}. \tag{3.32}$$

Here d denotes the wing span and SMC the standard mean chord which equals the chord length for a constant chord wing.

This results in the following expression for the propeller area

$$A_{prop} = \pi \left(\frac{3}{4}\right)^2 \frac{A}{\lambda}n, \tag{3.33}$$

where n denotes the number of rotors used for the VTOL structure.

3.3 Dynamic Models

To more accurately describe the launching sequence and to take into consideration control actions a simple dynamic model of the take-off was implemented using *Simulink* [31]. The flight path controller of this model is based on the one introduced by Rapp in his paper about VTOL of flexible AWE kites [13]. Simulations on different trajectories are carried out using different control strategies to investigate the influence of the aerodynamic force during take-off. The results can be used as a more precise estimation of the needed thrust and can be inserted in the mathematical model described in 3.2 for a more accurate sizing of the VTOL system.

In order to do so, two different dynamic models were implemented. One of them uses the attitude of the aircraft to align the propeller thrust T with the needed force F_{cmd} to follow the prescribed path. This is the conventional way multicopters are controlled. In this case, the aerodynamic force is not specially used but just occurs during flight like the gravitational force does. This model is called *multicopter controller* in this thesis.

In the second model, it is proposed that the aerodynamic force can optimally be used when aligning it with the needed force F_{cmd}. That way it is actually used to control the aircraft. In

order to use the rotors to produce the remaining thrust needed to equal F_{cmd}, tilting rotors are introduced in this model. This means the propellers can be rotated around the body frame's y-axis during flight. During the further procedure this approach is called *quadplane controller*.

In the following section, the principles used for both models are introduced before illustrating the differences in the two approaches. Both models require some important aircraft parameters. Namely, these are

1. Wing area A

2. Wing loading including VTOL system $w_{l,tot}$

3. Aerodynamic Characteristics $C_{L0}, C_{La}, C_{D0}, C_{Da}, M, \pm\alpha_0$

4. On-board power P_{ob}.

If using the models for design purposes, an estimation of the needed on-board power must be done using the previously described sizing tool. All further needed parameter values can be found in table 2.

3.3.1 Inputs to the Model

Wind

To guarantee a realistic wind environment, a wind shear model is assumed [32]. The wind velocity vector in B-frame $\left(v_{wind}^B\right)$ is calculated using the known wind speed in $6m$ altitude as well as the orientation of the aircraft and the current altitude $-z^O$. The model can be described by

$$v_{wind}^B = v_{6m} \frac{\ln\left(\frac{-z^O}{z_0}\right)}{\ln\left(\frac{6}{z_0}\right)}, \tag{3.34}$$

where v_{6m} is the wind speed at $6m$ height, z_0 is a constant equal to $0.05m$. For the reference speed v_{6m} a wind speed of $5\frac{m}{s}$ is assumed. In figure 7 the increasing wind speed at higher altitudes can be seen. The wind direction is again given using the wind angle λ_W.

Trajectory

The trajectory is defied in the same way as in the mathematical model above described in 3.2.1 by using an elevation angle ε and a desired path velocity $v_{path,k}$. If not stated other, ε is chosen to be 90° (vertical ascent) and $v_{path,k}$ is $1\frac{m}{s}$.

Orientation of Aircraft

Again, the yaw angle of the aircraft can be chosen but for the sake of an optimal use of the aerodynamic force it is proposed to always align the aircraft in wind direction heading into the wind. That way ψ is prescribed in the same way as in the model above. The remaining Euler angles ϕ and θ are determined during the computations and are used to track the desired force F_{cmd}, hence to control the aircraft as described in section 3.3.3. For the here introduced 2D models the roll angle ϕ can be set to zero.
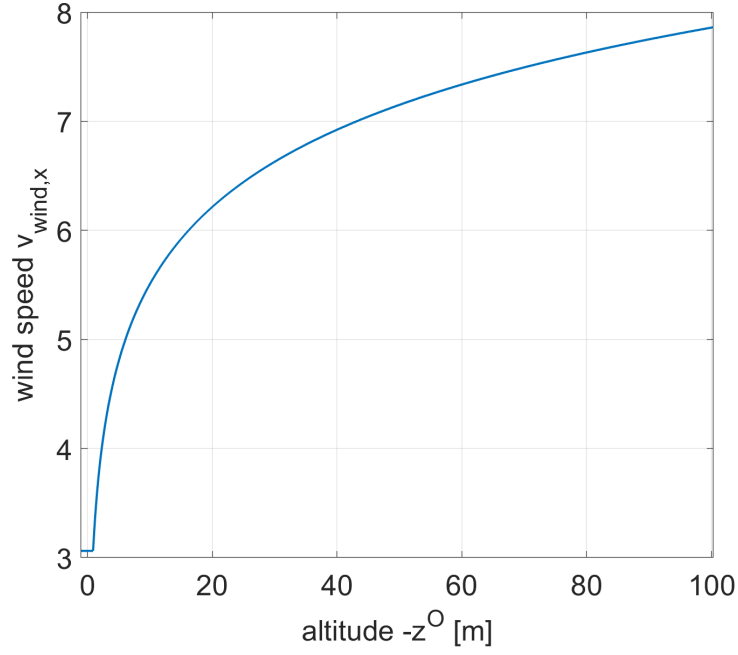
Figure 7: Wind shear model used for the dynamic models

3.3.2 Definition of Flight Path

For the controller to have a trajectory to follow, the flight path has to be parametrized and a target point has to be defined for each computing step. Since a rectilinear flight path is assumed for the launch of the system, a single waypoint X_w is necessary to describe the launching sequence and can be defined using the target height h_t and the elevation angle ε

$$X_w^W = \begin{pmatrix} \frac{h_t}{\tan(\varepsilon)} \\ 0 \\ h_t \end{pmatrix} \tag{3.35}$$

. When the starting point X_0 of the launch does not coincide with the ground station a relative representation of the flight path vector P_{fl} and the position of the aircraft X_{rel} has to be introduced.

$$P_{fl}^O = X_w^O - X_0^O \tag{3.36}$$

$$X_{rel}^O = X_k^O - X_0^O \tag{3.37}$$

Here X_k^O denotes the current position of the kite in the NED frame.

In order to calculate the target point on the path, the current position of the aircraft must be projected onto the flight path. The projected aircraft position X_{proj}^O is given by the normal projection described by

$$X_{proj} = \frac{\left(X_{rel}^O\right)^T P_{fl}^O}{\left(P_{fl}^O\right)^T P_{fl}^O} P_{fl}^O \tag{3.38}$$

. Now the target point X_{tar}^O on the trajectory can be defined by prolongate the projected aircraft

position along the flight path as

$$X_{tar}^O = X_0^O + \left(||X_{proj}^O||_2 + \delta_{sc} \right) \frac{P_{fl}^O}{||P_{fl}^O||_2}. \tag{3.39}$$

Here the scaling factor δ_{sc} is introduced as a tuning parameter that defines how aggressive the path tracking controller is. For $\delta_{sc} \rightarrow 0$ the aircraft will perpendicularly head to the flight path, which results in oscillations around the path. For a large δ_{sc} the kite will approach the flight path slowly. In the given model a scaling factor of $\delta_{sc} = 0.45$ was found to lead to satisfactory results. In order to avoid an overshoot of the target point at the and of the trajectory, the magnitude of the target point $||X_{tar}^O||_2$ is constrained to be smaller or equal to the magnitude of the waypoint $||X_w^O||_2$.

3.3.3 Flight Path Controller

The input to the control structure is the desired velocity $v_{cmd,k}^O$ to lead the aircraft to the flight path given in the NED frame. It can be computed using the target point, the position of the aircraft and the prescribed path velocity $v_{path,k}^O$ as follows

$$v_{cmd,k}^O = v_{path,k}^O \frac{X_{tar}^O - X_k^O}{||X_{tar}^O - X_k^O||_2} \tag{3.40}$$

.

A simple first order reference filter is used to attenuate fast inputs and therefore guarantee a feasible control output. The filter is defined by its time constant τ, which for high values attenuates a large range of the input, thus making the controller slower and vice versa. Thereby a proportional as well as an integrator feedback gain K_P and K_I are introduced. These can be used for tuning action when using different kites. In Addition, the integrator part guarantees to avoid steady state errors due to disturbances like the tether force. It uses the desired kinematic velocity $v_{cmd,k}^O$ and the current kinematic velocity v_k^O as inputs to compute the desired acceleration a_{cmd}^O and uses Newton's second law to determine a desired force F_{cmd}^O like

$$F_{cmd}^O = m\, a_{cmd}^O - F_g^O - F_a^O. \tag{3.41}$$

Here the models for the controlling approaches differ from each other. While for the multicopter controller the gravitational and the aerodynamic force are known and are given to the controller for an optimal performance, the aerodynamic force is included in F_{cmd}^O for the quadplane controller, thus not appearing in 3.3.3. Summing up, the path following controller is depicted in figure 8.

Now two different approaches are pursued to assemble this needed force F_{cmd}^O.

Multicopter Controller

Here the orientation of the aircraft is used to bring the rotors in the right position to equal F_{cmd}^O. Knowing the direction of the force required to track the flight path, the attitude set points for ϕ and θ can be determined using the fact that the propeller thrust must be directed along the

Figure 8: Simulink control structure of first order reference PI-controller

negative z-axis in body-fixed frame. This constraint can be written as

$$F_{cmd}^O = M_{OB} \begin{pmatrix} 0 \\ 0 \\ -||F_{cmd}||_2 \end{pmatrix} \tag{3.42}$$

. With the given transformation matrix M_{OB} relation can be solved for the roll and pitch angles, which leads to

$$\phi = -\arcsin\left(\frac{1}{||F_{cmd}||_2} \left(F_{cmd,x}^O \sin\psi - F_{cmd,y}^O \cos\psi \right) \right) \tag{3.43}$$

$$\theta = \arctan\left(\frac{1}{F_{cmd,z}^O} \left(F_{cmd,x}^O \cos\psi + F_{cmd,y}^O \sin\psi \right) \right). \tag{3.44}$$

In the model, no attitude control loop was implemented, thus the aircraft's orientation coincides with the resulting attitude set points and the propeller force F_P corresponds to the desired force in the body-fixed frame F_{cmd}^B. Following this approach, no rotor tilt is necessary.

Quadplane Controller

In contrast to the first version of the controller, the aircraft's attitude is not used to bring the propellers in the right position, but is defined when aligning the aerodynamic force with F_{cmd}^O. To do so, a different approach has to be introduced, where a set point for the angle of attack which defines the orientation of the aerodynamic force has to be found rather than set points for the attitude angles. First of all, the air-mass-referenced flight path angle γ_a and air-mass-referenced course angle χ_a have to be found in order to transform the given force vector into A-frame directly, which results in F_{cmd}^A. This is done using the known wind speed v_{wind}^O and the desired velocity $v_{cmd,k}^O$. By employing the wind triangle the desired airspeed $v_{cmd,a}^O$ can be found as [26]

$$v_{cmd,a}^O = v_{cmd,k}^O - v_{wind}^O. \tag{3.45}$$

Knowing the desired airspeed, the set points for the flight pass angle and course angle γ_a and χ_a can be found according to

$$\gamma_a = \arcsin\left(\frac{-v^O_{cmd,aero,z}}{||v_{cmd,aero}||_2}\right) \tag{3.46}$$

$$\chi_a = \arctan\left(\frac{v^O_{cmd,aero,y}}{v^O_{cmd,aero,x}}\right). \tag{3.47}$$

Now the desired force can be transformed into A-frame and by constraining the aerodynamic force to be aligned with the required one, the angle of attack α can be determined. This is done using the mathematical characteristic of two parallel vectors to have cross product equal to $\vec{0}$

$$F^A_{cmd} \times \begin{pmatrix} -F_D \\ 0 \\ -F_L \end{pmatrix} \equiv \vec{0} \tag{3.48}$$

. Employing this property and solving for the angle of attack yields

$$\alpha = \frac{C_{L0}F^A_{cmd,x} - C_{D0}F^A_{cmd,z}}{C_{Da}F^A_{cmd,z} - C_{La}F^A_{cmd,x}}. \tag{3.49}$$

For this computations, a first order approximation was done for both aerodynamic coefficient C_L and C_D. Now the relationship between the air-mass-referenced flight path angle, the angle of attack and the pitch angle can be used to determine θ accoring to

$$\theta = \gamma_a + \alpha. \tag{3.50}$$

Since it is proposed to always align the aircraft with the wind direction, the side slip angle β is assumed to be 0 as well as the roll angle ϕ. This is an accurate assumption because no acrobatic manoeuvres must be flown following a rectilinear flight path.

In order to generate the required force, the propeller thrust can be used. The remaining needed force can be computed like

$$F^B_{cmd,rem} = F^B_{cmd} - F^B_a. \tag{3.51}$$

Since the orientation of the aircraft is now defined by the angle of attack, an additional degree of freedom is needed to solve this problem. Here the concept of tilting rotors is introduced, where the rotor tilt angle ν is defined as a positive rotation around the body frame's y-axis as described in section 3.1.3. Here a similar procedure as for the attitude angles for the multicopter controller is chosen to solve for the rotor tilt angle. The rotor thrust is constrained to direct along the R-frame's negative z-direction. This can be represented by

$$F^B_{cmd,rem} = M_{BR} \begin{pmatrix} 0 \\ 0 \\ -||F_{cmd,rem}||_2 \end{pmatrix}, \tag{3.52}$$

where the transformation matrix M_{BR} contains to rotor tilt angle ν. It is now easy to solve for

ν which leads to

$$\nu = \arcsin\left(-\frac{F^B_{cmd,rem,x}}{||F_{cmd,rem}||_2}\right). \tag{3.53}$$

Now all the forces can be transformed into B-frame and the force balance can be set up.

3.3.4 Equations of Motion

This part is again valid for both the multicopter controller as well as for the quadcopter controller, since in both cases all forces are now known in the body-fixed frame. The only force acting on the aircraft which is not considered in the controller is the tether force F_T. Since the tether is not used for control actions the tether is assumed to be held loose, hence always directing to the ground. Therefore, the tether force consists only out of the gravitational force exerted on the chord. The mass of the tether is assumed to be $\frac{1}{40}$ of the aircraft's mass. Now the force balance can be written as

$$F^B_k = F^B_g + F^B_a + F^B_P + F^B_T, \tag{3.54}$$

where F^B_k is the resulting force acting on the kite.

After transforming the force into the NED-frame again Newton's second law can be used to determine the acceleration experienced by the aircraft. This acceleration is then integrated once to figure out the velocity v^O_k and a second time to compute the position X_k which then again is handed to the path planner to restart the cycle.

4 Results

The previously described models have been used to carry out parameter studies by varying all the input parameters and investigating their influence on the take-off procedure. The changes in the weight of the AWE system have been analysed in particular. In the following section the results of these evaluations are presented.

4.1 Parameter Studies using Static Model

The in section 3.2 introduced mathematical model was implemented in *Matlab* to evaluate the resulting on-board power and additional mass for varying parameters. That way, a guideline for the design of a VTOL structure including an estimation of the needed power, the size of the energy storage, a recommendation for the planned trajectory and the weight of the system is given. Additionally, the dependency of the additional mass coming from the launching system, is analysed for different setups and environmental conditions. For the computations the numerical solver *fsolve* was used [32].

Since a stationary ascent is investigated, it is supposed, that the rotors can be tilted in order to point upwards (in negative z-direction of O-frame) before take-off for each launching sequence, such that the proposed force balance in equation 3.29 remains valid. Further, the control actions required to balance disturbances, particularly coming from the wind, are not considered when evaluating the needed forces in this model. Finally, no analysis on the controllability is done, meaning it is assumed, that the prescribed trajectory and orientation of the aircraft can be tracked perfectly.

4.1.1 List of Parameters for Computations

In order to get representative results, it is important to chose feasible parameters for the evaluation. Therefore, values of relevant aircraft parameters were taken from the AWE prototype of the focusproject ftero MILENA which can be seen in figure 1. Table 2 shows the numerical values used.

The parameters that can be varied to minimize the needed rotor thrust and hover time and therefore find a lightweight solution for the VTOL structure are:

- Orientation of the aircraft ($\theta = 0°$ if not varied)

- Elevation angle ε ($\varepsilon = 90°$ if not varied)

- Path velocity ($v_{path,k} = 1\frac{m}{s}$ if not varied)

Since each of these parameters simultaneously influence the relevant parameters, namely thrust and hover time, evaluations on the sensitivity of the required on-board power are carried out independently for each variable.

Symbol & Value			Description
General Parameters			
v_{wind}	$=$	$5.5\frac{m}{s}$	wind speed
ρ	$=$	$1.225\frac{kg}{m^2}$	air density
g	$=$	$9.81\frac{m}{s^2}$	gravitational acceleration
h_t	$=$	$100m$	target height (suggested)
μ_p	$=$	$3.95\frac{kW}{kg}$	power density of power unit [19]
μ_e	$=$	$600\frac{kJ}{kg}$	energy density of batteries (lithium-ion polymere battery [27])
s	$=$	1.5	safety factor (suggested)
η	$=$	0.7	propeller efficiency
Aircraft Parameters (all taken from MILENA)			
A	$=$	$1.38m^2$	wing area
λ	$=$	10	aspect ratio
n	$=$	4	number of rotors
w_l	$=$	$10.65\frac{kg}{m^2}$	wing loading without VTOL system
$w_{l,tot}$	$=$	$13.71\frac{kg}{m^2}$	wing loading including VTOL system
C_{L0}	$=$	1.62	constant lift coefficient
C_{La}	$=$	$6.02\frac{1}{rad}$	first order lift coefficient
C_{D0}	$=$	0.105	constant drag coefficient
C_{Da}	$=$	$0.401\frac{1}{rad}$	first order drag coefficient
$\pm\alpha_0$	$=$	$25°/\text{-}20°$	cutoff angles of lift coefficient
M	$=$	15	transition rate of lift coefficient

Table 2: Considered parameters for numerical investigation of launching and landing sequence.

4.1.2 Effect of Lift Force

In a first step, the lift force acting on the aircraft during hovering is investigated. Since it strongly depends on the angle of attack it is expected, that the contribution of the lift to oppose the gravitational force can be influenced by the orientation of the aircraft, precisely by the pitch angle θ.

In figure 9a the drastic change of the aerodynamic force at varying pitch angles can be seen. At the given environmental conditions a maximal force in z-direction of $-78.3N$ is reached at a pitch angle of $\theta = 28.5°$. The lift force would achieve even higher values for a larger wing area or higher wind speeds.

In figure 9b the effect of the aerodynamic force on the needed thrust is shown. Thereby the decreasing mass plays an important role for the needed thrust and therefore intensifies the influence of the aerodynamic force. For the given aircraft, the required thrust decreases to 36.6% of the required one if neglecting the aerodynamic force. However, it must be kept in mind that the disturbing aerodynamic force in x-direction also reaches its maximum at this operating point, which means the forces needed for control actions are comparatively high and should not be neglected when sizing the energy storage.

In addition, it must be considered that negative values for F_a^O can be reached for negative pitch angles. This means, the aerodynamic force exerts additional down force on the aircraft which has to be compensated with propeller thrust.
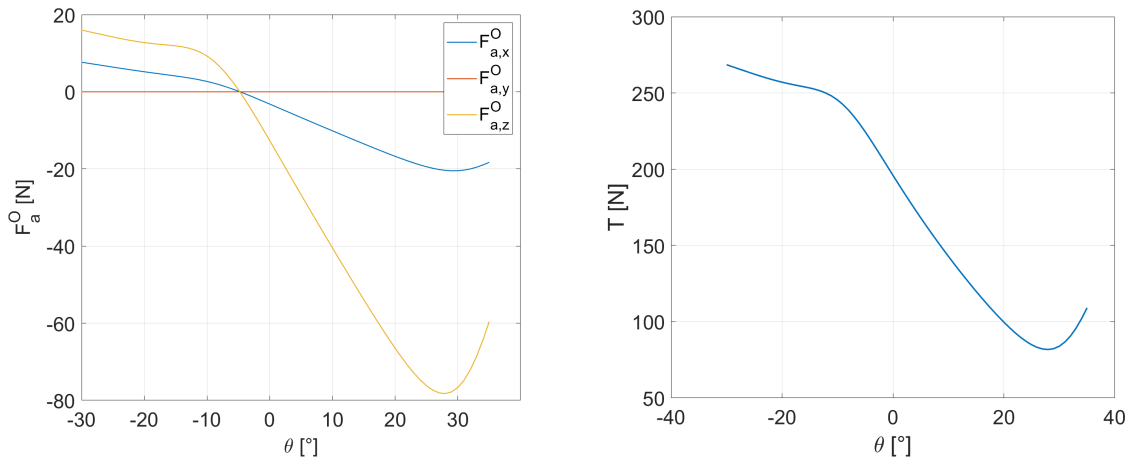
Figure 9: (a) Dependency of the aerodynamic force F_a^O on pitch, (b) change of thrust due to increasing lift force at varying pitch

4.1.3 Influence of Oblique Flow on Propeller Thrust

According to the expanded momentum theory in oblique flow the power required to produce a specific amount of thrust decreases for increasing propeller elevation angles, that is for large lateral wind speeds. (site oblique flow Theys). To evaluate the numerical impact of this effect the resulting thrust at different wind speeds is computed, neglecting aerodynamic forces and assuming constant power.

In Figure 10 the effect of an increasing lateral inflow velocity can be seen. For the operation of an AWE system wind gusts up to $20\frac{m}{s}$ must be expected. With the given expanded momentum theory in oblique flow this leads to beneficial thrust of $36.23N$ which corresponds to 7.03% of windless conditions. Such high wind speeds are not considered in the evaluation of the on-board power but the influence of oblique flow on the thrust is nonetheless considered throughout the computations.
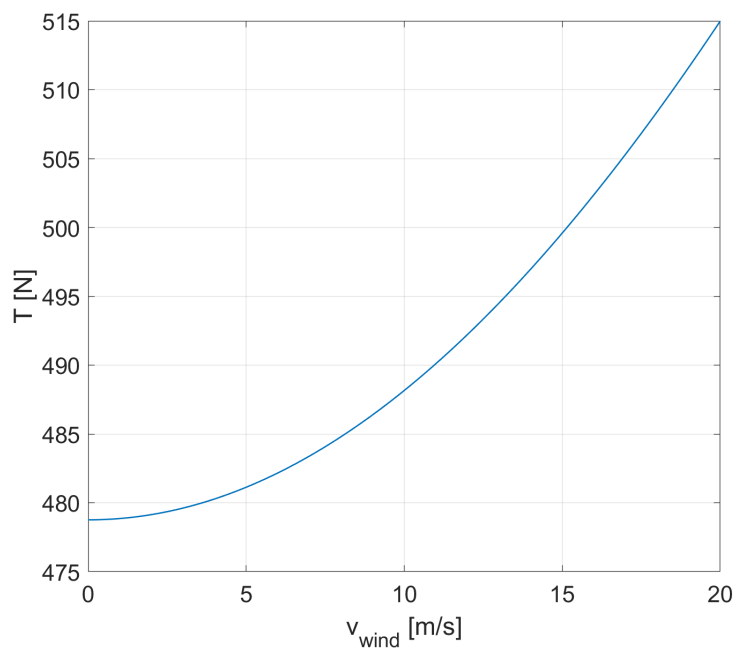

Figure 10: Propeller thrust depending on velocity of lateral inflow

4.1.4 Varying Orientation of Aircraft

In the previous section the enormous influence of the lift force on the needed thrust and it's dependency on the aircraft's orientation has been shown. The next step is to evaluate the savings that can be reached regarding the on-board power and the mass of the VTOL structure by utilizing the aerodynamic force.

The on-board power behaves analogue to the rotor thrust but reduces even more to remaining 20.12% of the power needed when neglecting the aerodynamic force. This can be seen in figure 11a The difference comes from the likewise decreasing induced velocity v_i that is required to compute the needed power according to equation 3.18.

With decreasing on-board power the mass of the VTOL system gets smaller as depicted in figure 11b. Since m_p, m_e and m_{vtol} all depend linearly on the on-board power, they all decrease to 20.12% of their original value. A total mass saving of $6.46kg$ can be reached which corresponds to 28.37% of the total mass, neglecting the aerodynamic force.
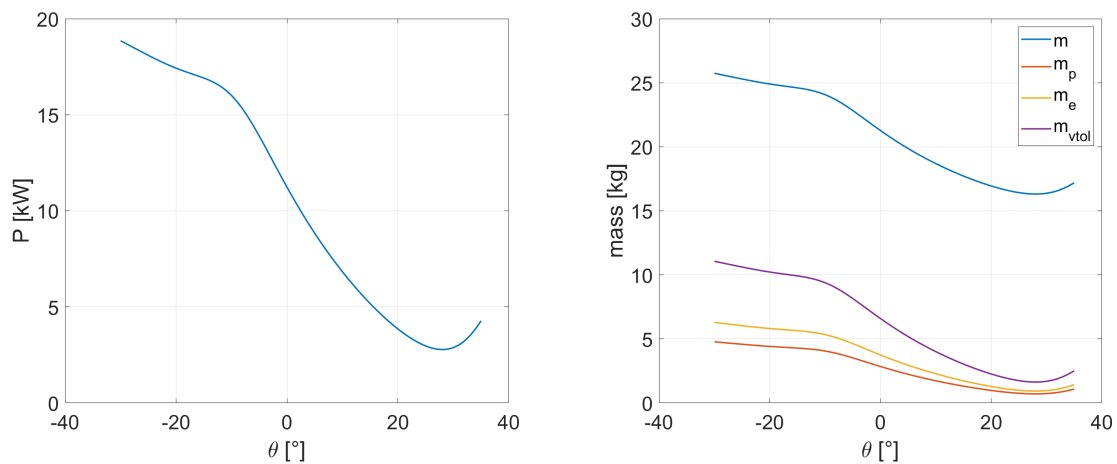

Figure 11: (a) Needed on-board power depending on pitch, (b) development of total mass and sub masses at varying pitch

4.1.5 Varying Path Velocity

When varying the advance velocity of the aircraft holding the other parameters constant, two main effects counteracting each other can be observed.

In figure 12a one can see that the aerodynamic lift gets smaller and even pushes the aircraft downwards for increasing path velocities. This is due to a significant change of the angle of attack. The flattening of the force's z-component for high advance velocities is due to the effect of stall since the angle of attack reaches strongly negative values. This effect gets smaller for higher wind speeds but is noticeable with the chosen one of $5.5\frac{m}{s}$. At an advance speed of approximately $1.5\frac{m}{s}$ the aerodynamic force disappears.

The second main effect comes from the significantly larger energy storage due to a longer flight time and therefore higher additional mass for very slow path velocities. This impact can be seen in figure 12b, where this influence is particularly important for slow advance speeds. Another principle that has a minor impact is the loss of thrust due to axial inflow at higher path velocities. This effect would counteract the effect of increasing mass for slow advance speeds but is little to have a significant impact.
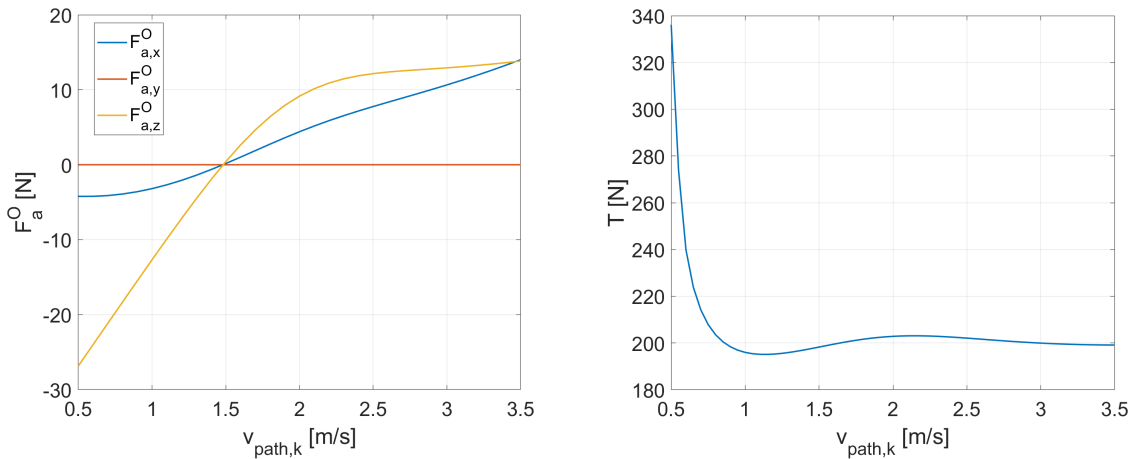
Figure 12: (a) Dependency of aerodynamic force F_L^O on varying path velocity, (b) thrust depending on varying path velocity

When evaluating the needed on-board power for different advance speeds one can see that a minimum is found for approximately $1.1\frac{m}{s}$, like it is shown in figure 13a. The significant increase of power for reduced path velocities is analogue to the thrust due to the increasing mass of the aircraft. Moreover, it can be noticed, that in contrast to the thrust the required power stays nearly constant after reaching a certain level when further increasing the advance speed. This can be explained by a larger difference of $v_i - w^B$ in equation 3.18, meaning the faster the aircraft is flying in rotor's direction, the more power is needed for a given thrust.

In figure 13b the previously described effect of a larger energy storage for a slow ascent due to the longer flight time. What's further interesting is the fact that the energy storage keeps becoming lighter for higher velocities whereas the power unit stays the same. The reason is that the flight time keeps decreasing, while the required on-board power remains constant. This means the VTOL structure keeps getting lighter for higher path velocities in this model and a minimal mass of $m_{vtol} = 4.21kg$ is reached at the maximal evaluated path velocity of $v_{path,k} = 3.5\frac{m}{s}$ However, similar to the solution for a minimal mass for the orientation of the aircraft, the disturbances and therefore the control actions become larger for higher advance velocities, making an arbitrary fast ascent unfeasible and inefficient.
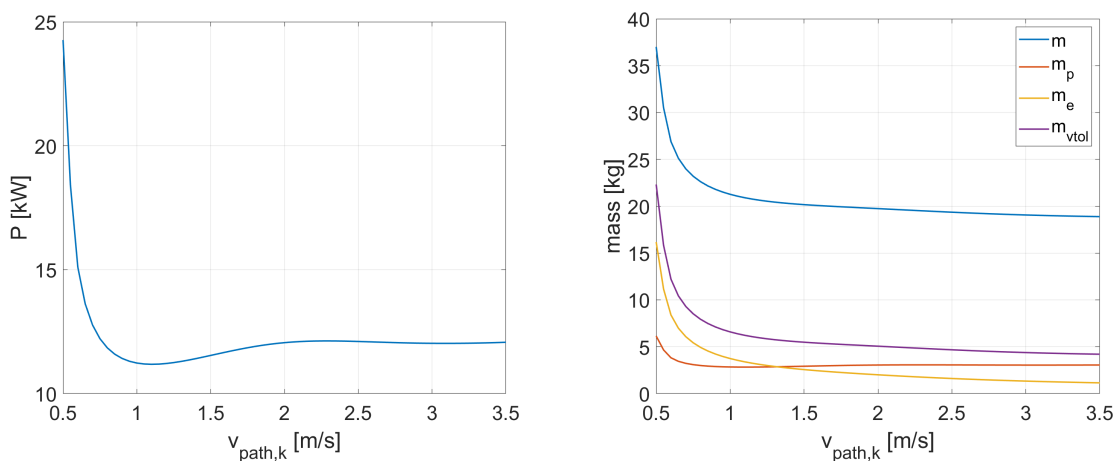

Figure 13: (a) Impact of path velocity on needed on-board power, (b) changing mass depending on varying path velocity

4.1.6 Varying Elevation Angle

Another parameter that can be used to optimize the launching sequence is the flight path, which is defined by the elevation angle ε. Since it describes the inclination angle of the linear flight path it has primarily an impact on the flight time and on the angle of attack.

Figure 14a shows how the aerodynamic force evolves at different elevation angles. The lift force always remains positive pointing in negative z-direction, meaning no strongly negative angles of attack are reached at any inclination angle. Nevertheless, it can be stated, that flying towards the wind (elevation angle $\varepsilon > 90°$) leads to a greater angle of attack as well as to an increased airspeed and therefore to a larger aerodynamic force. However, it does not achieve very high values and therefore the minimal needed thrust to equal the gravitational force is comparatively large with $187.2N$, meaning 16.2% of the originally needed thrust is compensated by aerodynamic forces as shown in figure 14b.
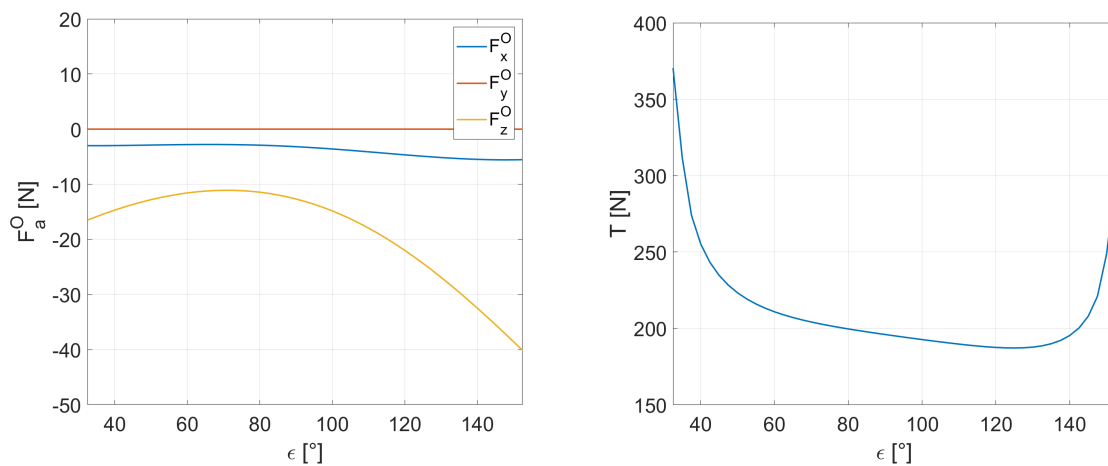

Figure 14: (a) Dependency of aerodynamic force F_L^O on varying elevation angle, (b) thrust at varying elevation angle

Since the airspeed at the rotors doesn't change remarkably, the effect of lateral in flow on the propeller efficiency can be neglected. Therefore, the plot in figure 15a describing the on-board power looks very similar to the one of the thrust. A minimal required power of $10.42kW$ is reached at an inclination angle of $125°$.

In figure 15b the resulting mass of the different sub systems is shown. Here, the significant influence of a longer hover time for extreme elevation angles, meaning flat trajectory, can be seen. Because the size of the energy storage increases before the propulsion unit gets larger, the minimum can be found at a smaller elevation angle of $105°$ and only $1.63kg$ of the original mass neglecting lift can be saved.

4.2 Results of Parameter Study

Based on the investigations done in the previous section, a suggestion of how to launch and land a AWE aircraft using the VTOL approach with propellers is made. In a last step, an estimation for the needed on-board power, the energy storage and thereby the associated mass of the launching structure is given.

The orientation of the aircraft has a major impact on the aerodynamic force and has therefore to be examined carefully. It could be shown, that a pitch angle of $\theta = 28.5°$, a maximal usable
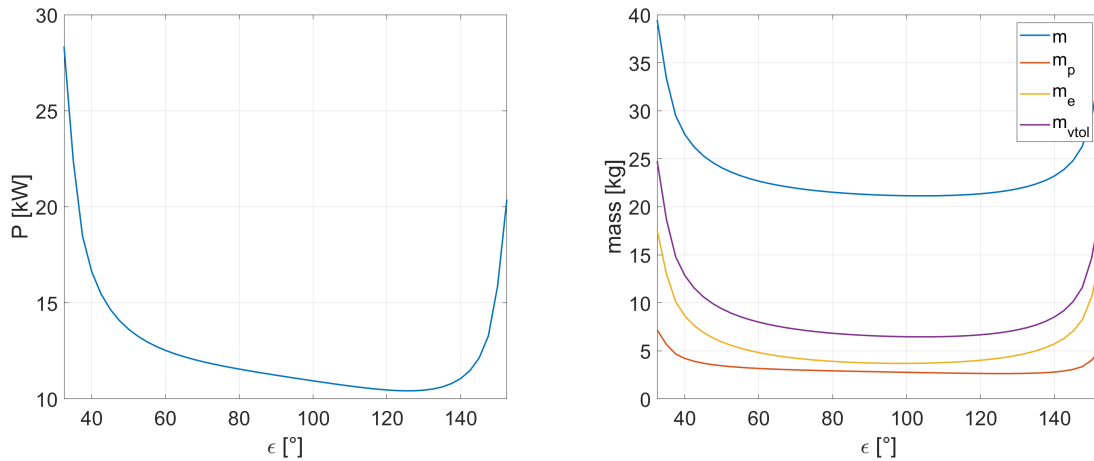
Figure 15: (a) Influence of elevation angle on needed on-board power, (b) Changing mass depending on elevation angle

lift force of $78.26N$ could be reached. This evaluation was done for a vertical flight trajectory with a path velocity of $v_{path,k} = 1\frac{m}{s}$. Since a small needed thrust leads to a lightweight system and this again needs even less thrust, the effect of an increasing lift force plays an important role. Just by finding the optimal orientation of the aircraft, the aircraft's mass could be reduced by $6.46kg$ which corresponds to 71.63% of the mass computed with default launching parameters. The drawback of the huge influence is, that it is sensitive to disturbances or to changes in wind speed. Therefore, when trying to maximize the aerodynamic force using the kite's orientation, a very reliable attitude controller to optimally track the prescribed pitch angle is needed. In addition, thrust and therefore the energy needed for control actions are not considered in this model. On the other hand, the assumed wind speed is rather small for the use of an AWE system and leads therefore to a more conservative result. For a more accurate estimation a dynamic model has to be considered, which is done in the second part of this thesis.

The effect of varying the advance speed can be analysed with less uncertainties, since it does not strongly depend on the aerodynamic force. The major impact of the advance speed applies to the hover time and therefore to the sizing of the energy storage. A too slow ascent results in a drastically enlarged energy storage which leads to a heavier system and therefore to more thrust needed. Again, this effect is self-reinforcing and therefore one has to pay attention not to be close to this range beginning at approximately $0.8\frac{m}{s}$. Although, the effect of the path velocity on the aerodynamic force is not as big as for the pitch angle, it can be stated, that a slower advance speed leads to higher lift forces due to a larger angle of attack. It can be seen, that the weight of the overall system gets smaller for increasing advance velocities, but again since controllability is not investigated, this can be misleading. Therefore, the advance speed should lie between $1\frac{m}{s}$ and $2.5\frac{m}{s}$ to guarantee an efficient and realizable ascent. Again a dynamic model can help to give a more accurate recommendation.

For the trajectory to fly it can be stated, that it is clearly more efficient to fly a flat trajectory in order to maximize the angle of attack and therefore the aerodynamic force. This effect can be amplified by flying into the wind and hence increase the airspeed. An optimal solution regarding the mass of the VTOL structure could be found at an elevation angle of $105°$, even though the mass saving of $1.63kg$ is rather small compared to the one optimizing the aircraft's orientation. Furthermore, it could be shown that the increasing hover time for very flat trajectories leads to

a drastically increasing mass of the storage system and therefore to a sub optimal system.

Overall, it could be shown, that utilizing the aerodynamic force for lift generation and thereby reducing the needed thrust, has a great potential to make the VTOL approach more viable for AWE systems. That way, the greatest weakness of this launching concept, the additional mass due to the motors and batteries, can be reduced significantly. The largest impact on the resulting mass of the launching system was found to be exerted by the orientation of the aircraft. The least potential to reduce the size of the VTOL system was found in the elevation angle of the flight path. An overview of the found optimal launching parameters and the mass savings reached can be found in 3.

The introduced model can be used to give an estimation of the needed power train and the capacity of the batteries for the VTOL system for any AWE kite, knowing the wing area, the kite's mass without launching system and the aerodynamic behavior. That way, the model can be used during the design phase for the sizing of the motors and the batteries. An overview of the procedure when determining the mass of the VTOL components is given in figure 16. The model also provides the basis for an optimal start sequence resulting in a minimal energy consumption. For a more accurate estimation the start sequence has further to be simulated with a dynamic model to account for control actions and feasibility of the obtained results.

Optimal Value	m_p	m_e	m_{vtol}	Δm_{vtol}
$\theta = 28.5°$	$0.7041kg$	$0.9271kg$	$1.6311kg$	$6.46kg$
$v_{path,k} = 2.5\frac{m}{s}$	$3.06kg$	$1.62kg$	$4.68kg$	$3.41kg$
$\varepsilon = 105°$	$2.73kg$	$3.73kg$	$6.46kg$	1.63kg

Table 3: Optimal flight path regarding minimal weight of the VTOL structure for each of the three parameters θ, $v_{path,k}$ and ε
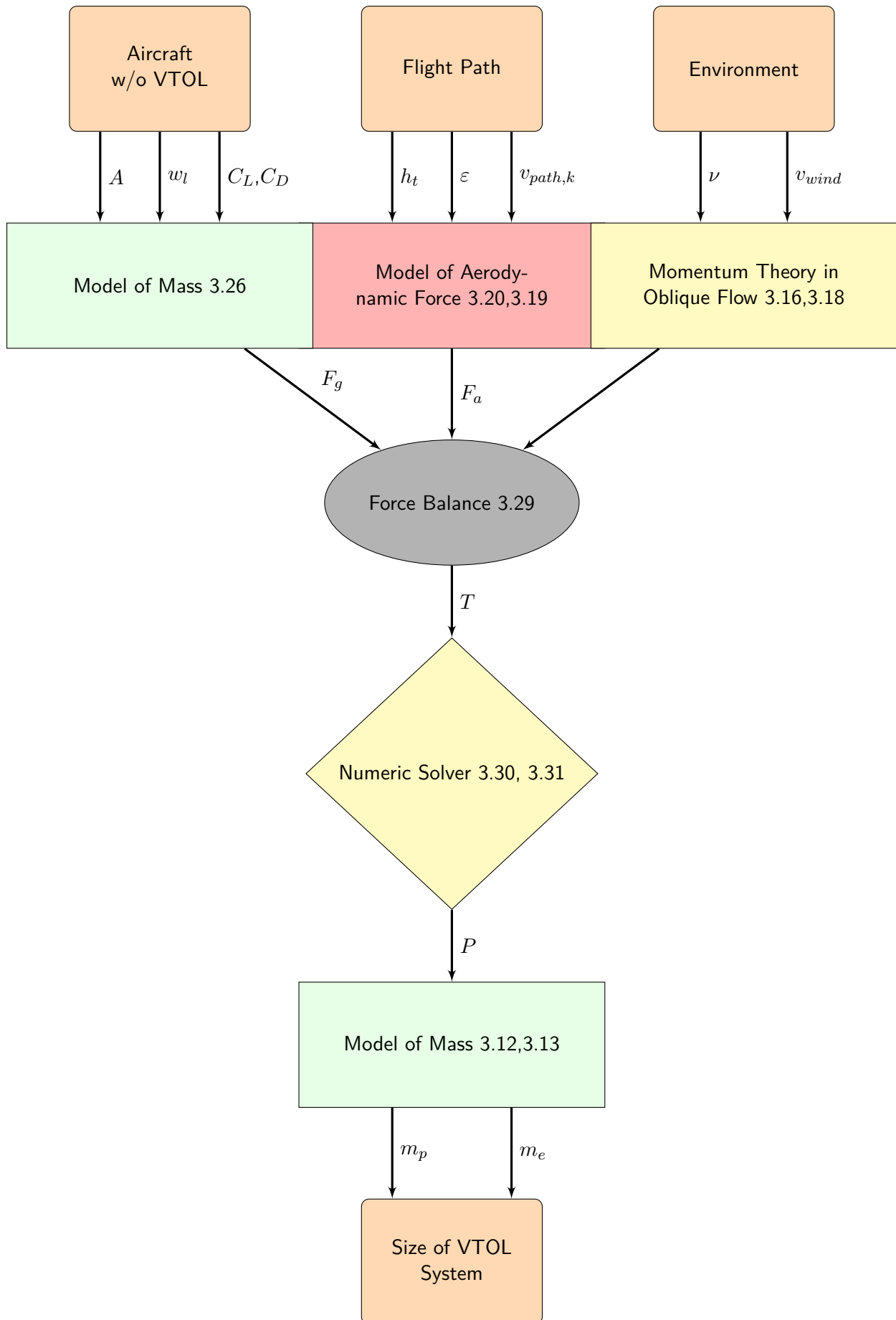
Figure 16: Methodology for determining size of the VTOL system for a given AWE aircraft.
Color code: orange: Inputs/Outputs; red: aerodynamic model; green: mass model; yellow: momentum theory ind oblique flow

4.3 Simulations of Different Launching Sequences

The dynamic models are used to perform simulations on the launching procedure for diverse strategies. Two parameters can be chosen in order to modify the take-off procedure. These are the elevation angle ε and the path velocity $v_{path,k}$. Numerous simulations were carried out to analyse the effect of both of the parameters on the thrust needed for launching, which again was used to investigate the required on-board power and size of the energy storage. If not stated other, a default elevation angle of $\varepsilon = 90°$ (meaning vertical flight path) and a path velocity of $v_{path,k} = 1\frac{m}{s}$ are chosen. A time constant of $\tau = 1s$ resulted in a good controller performance with few oscillations and realistic propeller forces. The results of these studies can be compared to the outcome of the analysis done in section 4.1. Furthermore, by using both introduced models a comparison between the two control strategies can be made and the potential of using the aerodynamic force for launching the aircraft is examined.

4.3.1 Parameter Study for Multicopter Control Approach

As described in section 3.3.3 the multicopter control approach represents the idea of using the aircraft's attitude to bring the rotors in the right position to generate the required force. Therefore, the attitude angles are predefined throughout the simulations. In figure 17a the roll and pitch angle during the ascent can be seen. In the first seconds small oscillations can be seen around the pitch axis. This effect is due to the large change in acceleration directly after take-off and can be reduced by choosing a higher time constant τ of the controller. In order to align the rotors with F_{cmd}, a negative pitch angle is required which reduces the angle of attack and therefore the aerodynamic force. The angle of attack is further strongly influenced by the advance velocity. This can be seen in figure 17b where the aerodynamic force increases significantly after reaching the desired target height because of a larger angle of attack. Moreover, the aerodynamic force increases during ascent because of the stronger blowing wind.
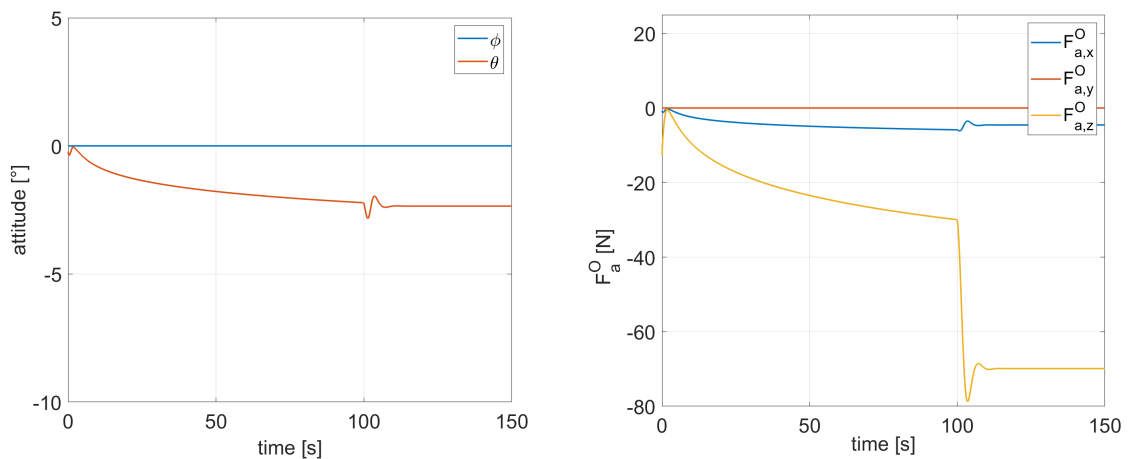

Figure 17: (a) Evolution of attitude angles during the ascent, (b) Changes in aerodynamic force during take-off

The change in thrust during take-off procedure can be seen in figure 18a. After reaching the maximum directly after take-off, the needed thrust gets smaller at higher altitudes. This is mainly due to the increasing aerodynamic forces coming from the stronger blowing wind. When reaching the waypoint the needed thrust decreases massively because of the larger aerodynamic

force coming from an increased angle of attack. Additionally, the required thrust for the evaluation of the static model described in section 3.2 is depicted. It can be seen, that the two models reveal nearly the same values right after the start. Since the wind speed stays constant for the static model, the thrust does not change during ascent.

The orientation of the forces occurring while launching as well as the aircraft's orientation are described by arrows in figure 18. Here the angle of elevation is chosen to be $\varepsilon = 110°$ in order to avoid overlapping arrows. Again the abruptly increasing aerodynamic force when reaching the target height can be recognized. Furthermore, it can be seen that the rotor force is decreasing while the aerodynamic force is getting larger during flight.
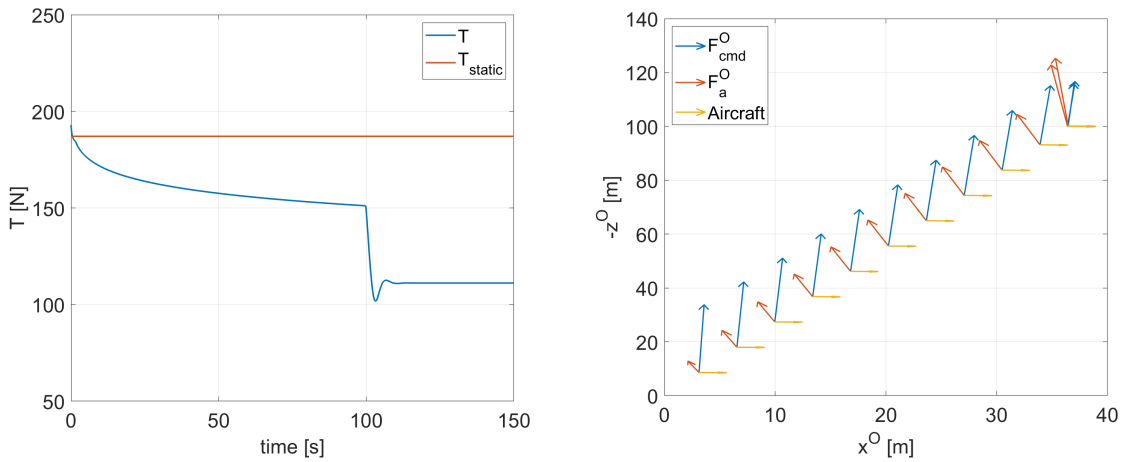

Figure 18: (a) Needed thrust during take-off sequence, (b) Orientation of the appearing forces

In a next step the dynamic model is used to investigate the influence of the chosen flight path and advance velocity on the needed thrust. That way, the potential of optimizing the launching strategy can be analysed. In order to do that, multiple simulations were carried out and with the computed propeller thrust the needed on-board power as well as the masses of the different subsystems are figured out.

Varying the Path Velocity

To compute the mass of the propulsion unit and the energy storage the model described in 3.1.5 was used. Thereby, the maximal occurring thrust was used to compute the mass of the power train, whereas the required energy for the launch was determined by summing up the energy used in each calculation step like

$$E_{tot} = \sum_{\delta t=0}^{t_{end}} 2P(t)\delta t, \tag{4.1}$$

which evolves to an integral for infinite small time steps δt. The factor 2 is to account for the landing procedure again. For the evaluation of different path velocities the elevation angle was kept constant at $\varepsilon = 90°$. The results, presented in figure 19a, show a similar behavior like the computations in section 4.1, whereas the mass of the propulsion unit increase at faster ascent speeds. This effect could not be identified in the previously performed calculations. Regarding the size of the energy storage a clear trend can be seen, where for slow path velocities a steep increase in needed energy emerges. Adding up the masses to the entire VTOL structure a minimum of $m_{vtol} = 4.88kg$ can be found at around $v_{path,k} = 2.5\frac{m}{s}$. This corresponds to a

mass reduction of $1.5kg$ or 23.5%

Varying the Elevation Angle

The same procedure was done for different elevation angles holding the flight velocity constant at $v_{path,k} = 1\frac{m}{s}$. Since the evaluations in section 4.1 have shown that it is favourable to fly into the wind the focus was put on elevation angles of $\varepsilon > 90°$. Doing so the relation shown in figure 19b emerged. It can be seen, that other than in the evaluation in section 4.1 the required power gets slightly larger with increasing elevation angle. Since the maximal occurring thrust is used to calculate the mass of the propulsion unit, the peak value directly after take-off is the decisive factor and can be reduced by using a larger time constant for the filter. Thus, the slightly changing mass of the propulsion unit is not considered as meaningful. The mass of the energy storage evolves as expected but for smaller elevation angles as for the static model. The minimum could be found at an elevation angle of approximately $92.5°$. A reason could lie in the control actions necessary to compensate the aerodynamic force in x-direction which was not considered in the static model. This way a larger aerodynamic force also leads to more control action and thus increasing thrust. The minimum represents a flight into the wind, which can be explained with a larger aerodynamic force compared to flying backwards with the wind. The results show the large influence of the flight time for extreme elevation angles, meaning flat flight paths. The minimal achieved mass of the VTOL structure is $m_{vtol} = 5.56kg$.
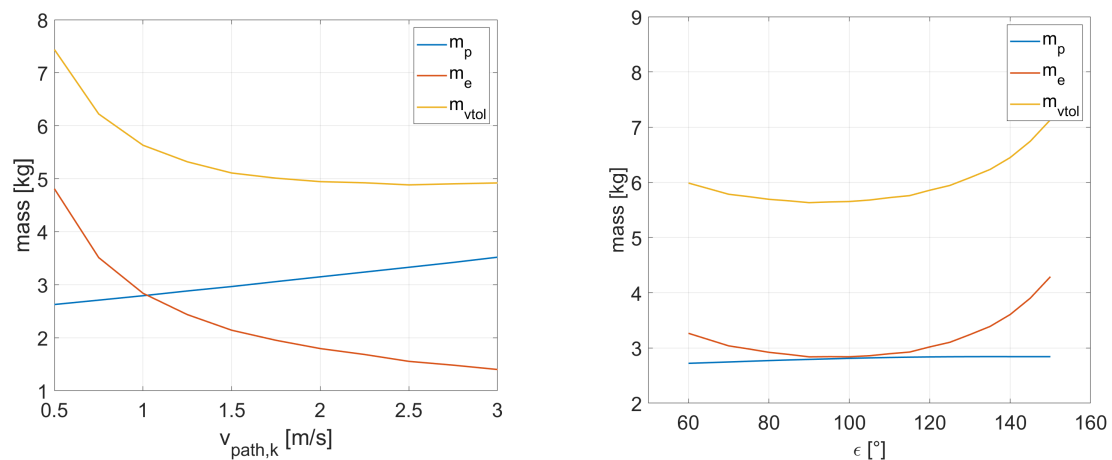

Figure 19: (a) Changing mass of launching structure depending on different advance velocities, (b) Masses of VTOL structure at varying elevation angle

The results of the simulations using the multicopter controller are showing similar trends and result in comparable values as the one calculated in the first part of the thesis. It can be stated that the assumptions made are feasible and the control actions do not require remarkably energy. In the evaluations executed in section 4.1 maximizing the aerodynamic force by orienting the aircraft in such a way that the angle of attack is maximized, was observed to have by far the largest impact on the needed thrust. Therefore, an alternative control approach is proposed, where it is tried to maximize the usage of the aerodynamic force while launching.

4.3.2 Parameter Studies for Quadplane Control Approach

As described in section 3.3.3 the idea is to enlarge the projection of the aerodynamic force on the desired force F_{cmd} in order to exploit the full potential of the lift force to reduce the needed

thrust. In a first step, it is proposed to align the aerodynamic force with the required one. Since both the gravitational as well as the tether force always point in positive z-direction of the NED frame the required force to compensate them directs upwards. In order to let the aerodynamic force point upwards a negative pitch angle is required as shown in figure 20a. This again leads to a negative angle of attack and reduces the aerodynamic force to a negligible value, as can be seen in figure 20b. Further, small oscillations can be seen after the aircraft reaches the desired target altitude, which can be explained with the abrupt deceleration. In this simple case where no further disturbances occur, the rotor tilt angle follows the pitch angle in reversed direction.
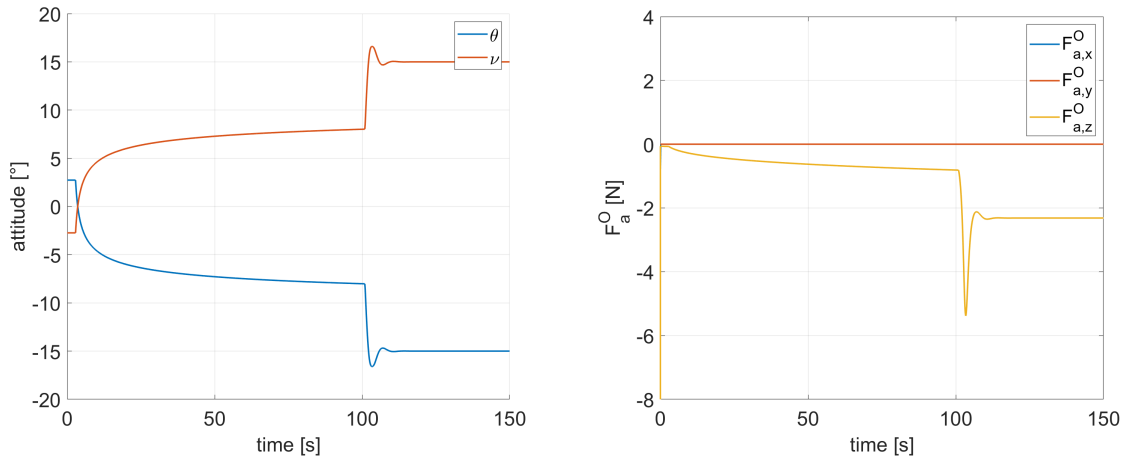

Figure 20: (a) Pitch and rotor tilt angle during ascent, (b) very small aerodynamic forces due to negative angle of attack

As a consequence of the small aerodynamic force, the required thrust remains nearly constant during take-off (figure 21a). The only deviation occurs after reaching the target height according to the short increase of the lift force. In figure 21 the orientation of the forces and the attitude of the aircraft are depicted, where the short peak of the aerodynamic force at a height of $100m$ can be observed. This plot is representing the situation for a elevation angle of $\varepsilon = 110°$.
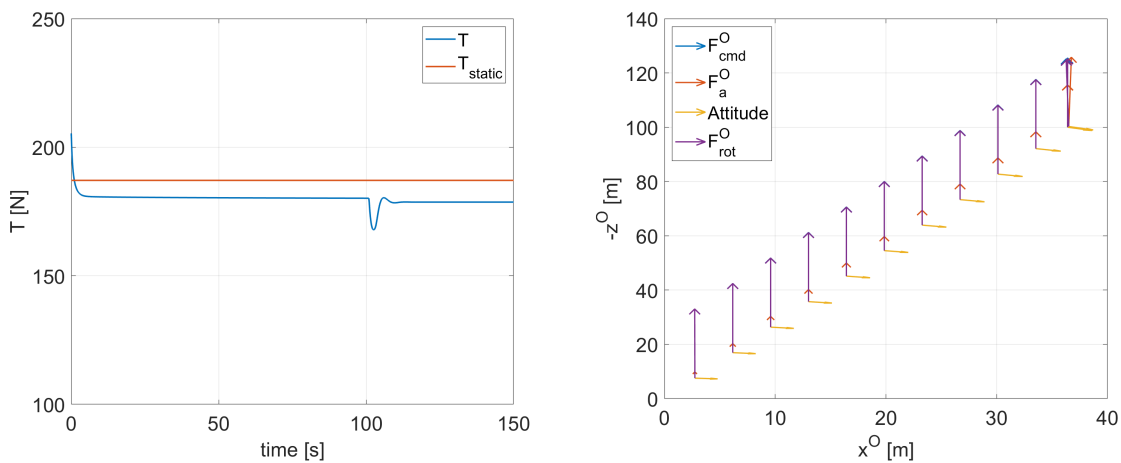

Figure 21: (a) Rotor thrust required during ascent, (b) orientation of forces and aircraft during launch

When analysing the required thrust for different elevation angles and path velocities the same trends as shown in section 4.1 can be detected. For advance velocities of more than $v_{path,k} = 2.5\frac{m}{s}$ the simulation gives unfeasible results for the required thrust at the end of the ascent,

because the overshoot gets very large. This effect puts a constraint on the possible advance velocity using this controller and can be seen in figure 22.
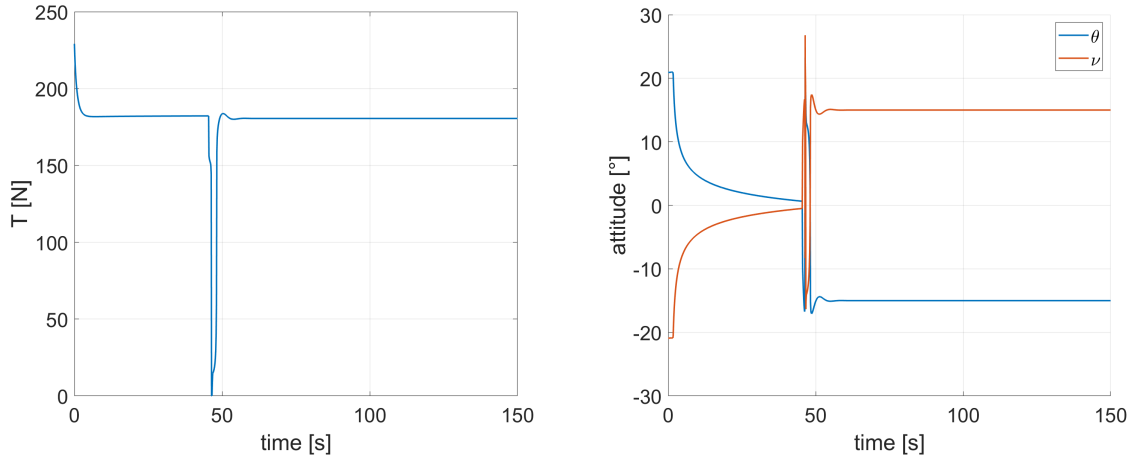

Figure 22: The large overshoot in thrust and in attitude angles at the end of the flight path.

Since the thrust remains nearly constant near the maximum, no significant savings regarding the mass of the VTOL structure can be reached. The results of varying the elevation angle even lead to a slightly higher mass as for the reference flight with $\varepsilon = 90°$ and $v_{path,k} = 1\frac{m}{s}$. This is because the flight time of the reference flight carried out with the multicopter controller was shorter and therefore a smaller energy storage is required. The reason for the longer flight time lies in the controller performance and can be adjusted with the time constant of the filter.

When varying the path velocity the expected trends shown in figure 23 emerged. The values reached are the same as for the multicopter controller, meaning a minimal mass of the launching system of $m_{vtol} = 4.88 kg$ could be reached.
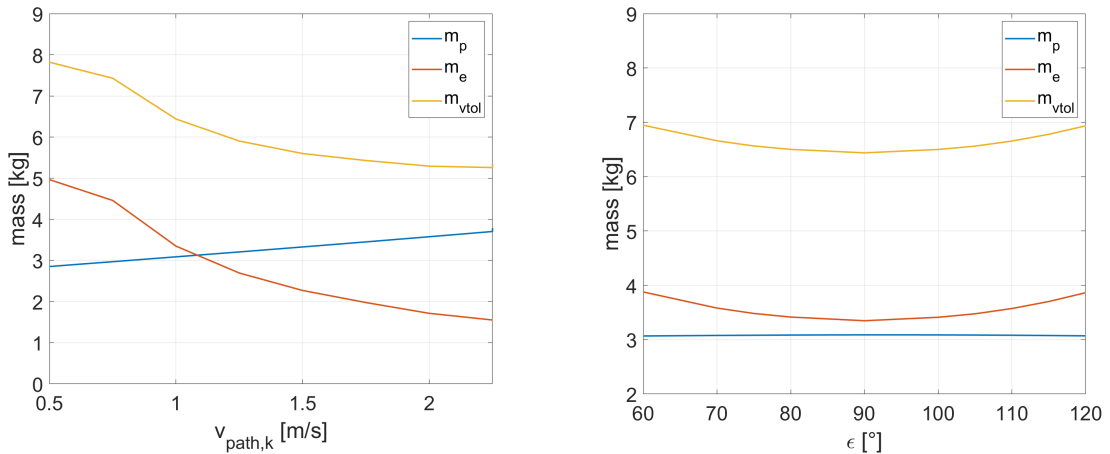
Figure 23: Changes of the mass of the propulsion unit and the energy storage during launch depending on elevation angle and path velocity.

4.3.3 Regulating Angle of Attack using Quadplane Controller

Since the aerodynamic force nearly vanished due to the strongly negative angle of attack, it is proposed to define constrains and give set points for the angle of attack in such a way, that the lift force still reaches high magnitudes. With the quadplane control approach introduced in

section 3.3.3 it is possible to regulate the angle of attack in a desired way. In the scope of this thesis it was not possible to introduce a method how to maximize the projected aerodynamic force in the direction of the required control force F_{cmd}, but some computations giving different angles of attack as set point have been conducted to give a sense on the potential of regulating the aerodynamic force to maximize its contribution for hovering.

As expected, the aerodynamic force increases significantly when enlarging the angle of attack. As a consequence the thrust can be reduced during flight which leads to way less energy consumption and way smaller batteries can be chosen. The relation between mass of the VTOL system and the angle of attack during the launch is depicted in figure 24a. At an angle of attack of $\alpha = 15°$ the minimal mass of the VTOL structure of $m_{vtol} = 3.8 kg$ could be reached, which corresponds to a mass saving of 40.42%. At higher angles of attack the simulation diverges because of large oscillations. It can further be seen, that the maximal needed thrust is not reduced significantly and even rises again with larger angles of attack. The reason is, that the maximal required thrust occurs direct after take-off and can therefore not be reduced remarkably with the aerodynamic force.

In figure 24b an example of the developing aerodynamic force during launching at a large angle of attack of $\alpha = 7.5°$ is given. Fast oscillations in z-direction occur which can possibly origin in the large disturbing forces in x-direction of the NED-frame coming from the aerodynamic force. It indicates the difficult controllability of the aircraft orientation. The oscillations could be reduced with a better attitude controller.
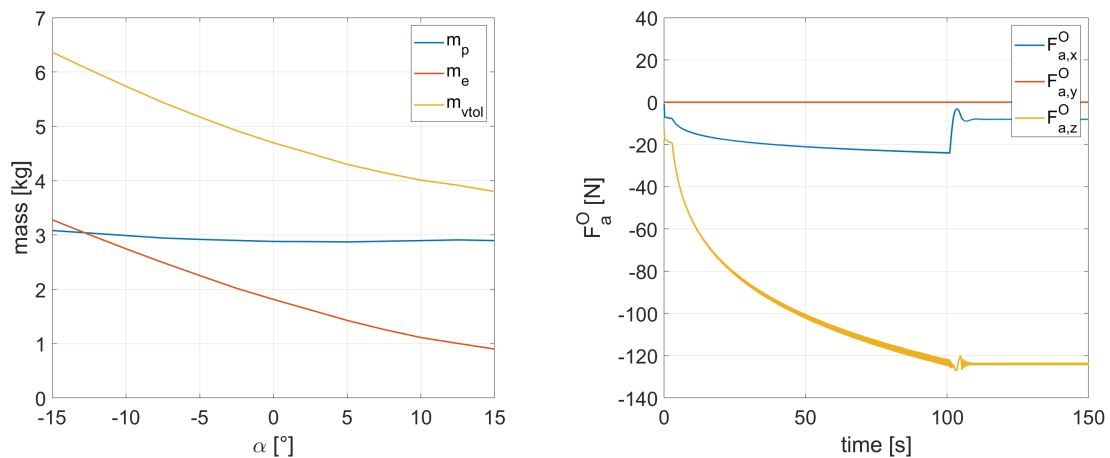

Figure 24: (a) Changing mass of VTOL structure when varying angle of attack, (b) increasing aerodynamic force at angle of attack $\alpha = 7.5°$

4.4 Results of Simulations on Different Launching Sequences

In order to investigate the VTOL concept with rotors more accurately for the use in AWE power plants, numerous dynamic simulations using a simple 2D model have been carried out. Thereby different launching strategies have been analysed by varying the elevation angle of the rectangular flight path and the path velocity regarding the impact on the needed thrust and consequently the size of the propulsion unit as well as the energy storage required for the take-off.

The results of the simulations reinforce the trends seen in the evaluation of the stationary ascent conducted in section 4.1. Although, the values can not be compared to each other

directly, since for the simulations the mass of the AWE aircraft including the VTOL structure has to be given. This mass was taken from MILENA again and lies with $m_{tot} = 18.92kg$ beneath the one calculated in the first section neglecting the aerodynamic force. This way, the mass of the entire system is given and only the mass reduction of the VTOL structure can be analysed.

For the multicopter control approach, where the aerodynamic force is not specifically regulated, a minimal required mass of the VTOL structure of $m_{vtol} = 5.56kg$ could be found at an elevation angle of $\varepsilon = 92.5°$. This corresponds to a mass saving of $0.82kg$ respectively 12.8% of the VTOL structure required neglecting the aerodynamic force. When varying the path velocity for the same control approach a minimal mass of $m_{vtol} = 4.88kg$ was found for the fast ascent speed of $v_{path,k} = 2.5\frac{m}{s}$. It can be stated, that the path velocity has a greater potential to reduce the launching structure's mass than the elevation angle, although it must be considered that a high path velocity requires a sophisticated controller to be realizable.

The same investigations were conducted for the quadplane control approach, where the aerodynamic force is regulated in order to be used for control purpose. When aligning the aerodynamic force with the required force F_{cmd} very small mass savings could be reached. In the case of varying the elevation angle no mass reduction was possible, because the aerodynamic force decreased to negligible values. When varying the path velocity, a decreased mass was reached for the highest evaluated velocities. At the advance velocity of $v_{path,k} = 2.5\frac{m}{s}$, a mass saving of $1.5kg$ could be realized. For faster ascents the overshoot at the end of the path leads to unrealistic results.

Since the results of the quadplane control approach were unsatisfactory and in order to analyse the potential of maximizing the aerodynamic force, some simulations regulating the angle of attack to a fixed value were conducted. It could be shown, that large mass savings $2.58kg$ are possible. However, to maintain such an aircraft orientation large control actions are necessary and an advanced attitude controller is needed.

Optimal Value	m_p	m_e	m_{vtol}	Δm_{vtol}
Multicopter Control Approach				
$v_{path,k} = 2.5\frac{m}{s}$	$3.33kg$	$1.55kg$	$4.88kg$	$1.50kg$
$\varepsilon = 92.5°$	2.82	$2.73kg$	$5.56kg$	$0.82kg$
Quadplane Control Approach				
$v_{path,k} = 2.5\frac{m}{s}$	$3.33kg$	$1.55kg$	$4.88kg$	$1.50kg$
$\varepsilon = 92.5°$	$3.09kg$	$3.34kg$	$6.43kg$	$-0.05kg$
$\alpha = 15°$	$2.89kg$	$0.90kg$	$3.80kg$	$2.58kg$

Table 4: Minimal mass of VTOL components for different flight paths

5 Conclusion

In this thesis, the VTOL approach of launching an AWE aircraft was investigated. A guideline for the design of a VTOL system for a given kite was introduced. Important aircraft parameters as well as the desired flight path can be given as an input to determine the required on-board power and the size of the energy storage. These can then be used as a reference for the selection of the motors, batteries, propellers and ESCs. This methodology can be applied for a preliminary sizing of the required VTOL components and facilitate the design of such a launching system.

Since the additional mass coming from the take-off structure is a weakness of this take-off concept, particular attention was paid to possibilities to minimize the weight of the aircraft. In order to do this, the aerodynamic force was included in the models and different possibilities to maximize its contribution to compensate the gravitational force were analysed. Thereby a maximal weight reduction of the VTOL components of 79.88% could be reached in the optimal case of a stationary ascent neglecting control actions. In order to reach such a lightweight solution extreme aircraft orientations must be maintained, which require either significant rotor input which consumes energy or an on-board system that enables to maintain a given attitude not requiring notable amounts of energy. For instance, a slider adjusting the aircraft's mass distribution could be such a solution. Nevertheless, the results of the investigations done in this thesis show the potential of using the aerodynamic force for the launch of AWE systems. These considerations are the basis for further researches in the major topic of how to launch an AWE kite most efficiently using the VTOL approach.

By analysing the effect of different rectilinear flight paths and the path velocity on the size of the VTOL structure, a recommendation for the take-off strategy is given. It has been shown, that heading into the wind with an elevation angle of approximately $\varepsilon = 92.5\text{-}105°$ and a path velocity of $v_{path,kin} = 2\text{-}2.5\frac{m}{s}$, leads to the most efficient start procedure. These results can be used from the numerous AWE companies that exploit the VTOL concept to realize a more efficient take-off procedure.

An approach to maximize the projection of the aerodynamic force in the direction of the required force was introduced. It could be shown, that since the aerodynamic force nearly vanishes for strongly negative angles of attack, aligning it perfectly with the required force leads to unsatisfactory results. Nevertheless, by regulating the angle of attack during the start procedure, it could be shown that using the aerodynamic force for control purposes has a great potential to minimize the size of the required VTOL construction. Taking this potential into consideration when designing controllers for the described launching procedure, novel control approaches could lead to a significantly more efficient take-off.

6 Outlook

The proposed design guideline can be used for preliminary sizing considerations when designing a VTOL system for an AWE kite. The exact choice of the power train has not been considered in this work. In a next step, a guideline or even an optimization of the respective components of the VTOL structure could be developed. This would require a market survey and large databases, but would simplify the design procedure.

In this thesis the great potential of using the aerodynamic force to minimize the propeller input during the launching sequence could be shown. The influence of different parameters has been investigated and each was analysed regarding the optimal configuration. In further studies, a global optimization of this problem could be conducted, aiming at minimize the additional on-board mass due to the VTOL components. An important goal of this optimization is to maximize the projection of the aerodynamic force in the direction of the needed thrust. Various considerations that were discussed in this thesis could lead to large improvements of AWE systems regarding their efficiency.

Another approach of minimize the additional mass of the AWE kite due to the launching construction could be a detachment of the VTOL framework after reaching the desired target height. This way the optimization of the take-off maneuver would be unnecessary. The major challenge is the complexity of this concept in particular of the landing.

In the second part of the thesis a control approach was proposed where the aerodynamic force is used for regulation. The introduced approach has not been successful. Nonetheless, trying to make full use of the lift force while starting, offers room for different interesting control approaches. The goal could be to use the aerodynamic force to compensate the gravitational one and to only need the propellers for control purposes. In a further study, one could aim to utilize the tether or on-board sliders to control the orientation of the aircraft instead of using the rotors which consume a lot of energy.

Bibliography

[1] "EnerKite." https://www.enerkite.de/. Eingesehen am 25.07.19.

[2] "Ampyx Power." https://www.ampyxpower.com/. Eingesehen am 24.07.19.

[3] "Twingtec." http://twingtec.ch/de/. Eingesehen am 24.07.19.

[4] "Makani Power." https://makanipower.com/. Eingesehen am 25.07.19.

[5] R. Schmehl, *Airborne Wind Energy: Advances in Technology Development and Research*. 2013.

[6] C. Loyd, Miles L. (Lawrwrence Livermore Nationa Laboratory, Livermore, "Crosswind Kite Power.," *Journal of energy*, vol. 4, no. 3, pp. 106–111, 1980.

[7] L. Fagiano and M. Milanese, "Airborne Wind Energy: An overview," in *2012 American Control Conference (ACC)*, pp. 3132–3143, IEEE, 2014.

[8] A. Cherubini, A. Papini, R. Vertechy, and M. Fontana, "Airborne Wind Energy Systems: A review of the technologies," 2015.

[9] R. Bättig, M. Hensen, B. Kader, M. Macuglia, J. Mark, M. Pagani, P. Sigron, and C. Zemp, "Endbericht Fokusprojekt ftero," 2019.

[10] L. Fagiano and S. Schnez, "On the take-off of airborne wind energy systems based on rigid wings," *Renewable Energy*, vol. 107, pp. 473–488, 2017.

[11] E. Bontekoe, "Up! How to Launch and Retrieve a Tethered Aircraft," 2010.

[12] L. Fagiano, E. Nguyen-Van, F. Rager, S. Schnez, and C. Ohler, "Autonomous Takeoff and Flight of a Tethered Aircraft for Airborne Wind Energy," *IEEE Transactions on Control Systems Technology*, vol. 26, no. 1, pp. 151–166, 2018.

[13] S. Rapp and R. Schmehl, "Vertical Takeoff and Landing of Flexible Wing Kite Power Systems," *Journal of Guidance, Control, and Dynamics*, vol. 41, no. 11, pp. 2386–2400, 2018.

[14] U. Ahrens, M. Diehl, and R. Schmehl, "Airborne Wind Energy," *Green Energy and Technology*, no. January, 2013.

[15] "Kitemill." http://www.kitemill.com/. Eingesehen am 25.07.19.

[16] "e-kite." http://www.e-kite.com/. Eingesehen am 24.07.19.

[17] "KiteX." https://kitex.tech/. Eingesehen am 24.07.19.

[18] A. Papageorgiou, M. Tarkian, K. Amadori, and J. Ölvander, "Multidisciplinary design optimization of aerial vehicles: A review of recent advancements," *International Journal of Aerospace Engineering*, vol. 2018, 2018.

[19] W. Ong, S. Srigrarom, and H. Hesse, "Design Methodology for Heavy-Lift Unmanned Aerial Vehicles with Coaxial Rotors," vol. 9781624105784, no. January, pp. 7–11, 2019.

[20] Ø. Magnussen, M. Ottestad, and G. Hovland, "Multicopter design optimization and validation," *Modeling, Identification and Control*, vol. 36, no. 2, pp. 67–79, 2015.

[21] X. Dai, Q. Quan, J. Ren, and K.-y. Cai, "An Analytical Design Optimization Method for Electric Propulsion Systems of Multicopter UAVs with Desired Hovering Endurance," *IEEE/ASME Transactions on Mechatronics*, vol. PP, no. January, p. 1, 2019.

[22] A. U. Zgraggen, L. Fagiano, and M. Morari, "Real-time optimization and adaptation of the crosswind flight of tethered wings for airborne wind energy," *IEEE Transactions on Control Systems Technology*, vol. 23, no. 2, pp. 434–448, 2015.

[23] G. Licitra, A. Burger, P. Williams, R. Ruiterkamp, and M. Diehl, "Optimum experimental design of a rigid wing AWE pumping system," *2017 IEEE 56th Annual Conference on Decision and Control, CDC 2017*, vol. 2018-January, no. Cdc, pp. 4018–4025, 2018.

[24] R. Brockhaus, W. Alles, and R. Locker, *Flugregelung*. Springer Verlag, Berlin Heidelberg, 3. auflage ed., 2011.

[25] B. L. Stevens, F. L. Lewis, and E. N. Johnon, *AND SIMULATION AIRCRAFT CONTROL Third Edition Dynamics , Controls Design , and.* John Wiley & SOns. Inc., Hoboken, New Jersey, 2016.

[26] R. W. Beard and T. W. McLain, *Small Unmanned Aircraft; Theory and Practice*. New Jersey: Princeton University Press;2012, 2012.

[27] P. Saenger, N. Devillers, K. Deschinkel, M. C. Pera, R. Couturier, and F. Gustin, "Optimization of Electrical Energy Storage System Sizing for an Accurate Energy Management in an Aircraft," *IEEE Transactions on Vehicular Technology*, vol. 66, no. 7, pp. 5572–5583, 2017.

[28] H. Martin, "Electric Flight - Potential and Limitations," *AVT-209 Workshop, Lisbon*, pp. 1–30, 2012.

[29] B. W. T. P. S. U. D. o. A. E. McCormick, *Aerodynamics, Aeronautics and Flight Mechanics*. No. 1, 1995.

[30] "XFLR5." http://www.xflr5.com. Eingesehen am 25.07.2019.

[31] "Simulink." https://ch.mathworks.com/products/simulink.html. Eingesehen am 24.07.19.

[32] "Matlab." https://ch.mathworks.com/help/matlab/. Eingesehen am 24.07.19.